

Metamorphic and Structural Evolution of the Southern Shackleton Range during the Ross Orogeny

By Werner Buggisch*, Georg Kleinschmidt†, Hans Kreuzer‡ and Stefan Krumm*

Summary: The Shackleton Range can be divided into three major units: (1) The East Antarctic Craton and its sedimentary cover (Read Group and Watts Needle Formation), (2) the allochthonous Mount Wegener Nappe (Mount Wegener Formation, Stephenson Bastion Formation, and Wyeth Heights Formation), and (3) the northern belt (basement: Pioneer and Stratton Groups, sedimentary cover: Haskard Highlands Formation (allochthonous?), and Blaiklock Glacier Group). The northern units are thrust over the southern ones. The thrusting is related to the Ross Orogeny.

The Mount Wegener Nappe, which appears to be a homogeneous tectonic unit, consists of a Precambrian basement (Stephenson Bastion Formation, Wyeth Heights Formation?) and a Cambrian cover (Mount Wegener Formation).

Some questions are still open for discussion: the position of the Haskard Highlands Formation (trilobite shales) may be erratic or represent a tectonic sliver, the relation of the former Turnpike Bluff Group, the origin of the crystalline basement west of Stephenson Bastion and others.

Zusammenfassung: Die Shackleton Range kann in drei größere Einheiten untergliedert werden: (1) den ostantarktischen Kraton und seine sedimentäre Überdeckung (Read Group und Watts Needle Formation), (2) die allochthone Mount Wegener Decke (Mount Wegener Formation, Stephenson Bastion Formation, Wyeth Heights Formation) und (3) die nördliche Shackleton Range (mit dem Basement der Pioneer und Stratton Gruppe und der Überdeckung der fraglich allochthonen Haskard Highlands Formation und der Blaiklock Gletscher Gruppe. Die nördlichen Einheiten sind während der Ross Orogenese über die südlichen überschoben worden.

Die Mount Wegener Decke, die tektonisch homogen erscheint, besteht aus einer präkambrischen Basis (Stephenson Bastion Formation und Wyeth Heights Formation?) und einer kambrischen Überdeckung (Mount Wegener Formation).

Einige Fragen sind noch offen, z.B. die Stellung der Haskard Highlands Formation (als erratische Einheit oder als tektonischer Span?), die Beziehung der Anteile der Turnpike Bluff Gruppe zueinander, die Natur des kristallinen Basements westlich der Stephenson Bastion und andere.

1. INTRODUCTION

In order to investigate the structure and metamorphism of the southern Shackleton Range crucial sections known from the literature were examined during the German GEISHA expedition, e.g., Watts Needle (MARSH 1983a), Nicol Crags and Mount Wegener (CLARKSON 1983, GRIKUROV & DIBNER 1979, PAECH et al. 1991). A survey of the former Turnpike Bluff Group was made at as many outcrops as could be visited during the field season. For the stratigraphic results of these investigations see

BUGGISCH et al. (1994). Furthermore, the northern boundary between the Read Group and the Mount Wegener Formation (formerly called at that place Flett Crags Formation) was mapped in detail (Fig. 2). Each nunatak of this critical area was visited by helicopter. The northern boundary between the Wyeth Heights Formation (formerly part of Turnpike Bluff Group) and the northern crystalline basement (Pioneer and Stratton Groups) was studied in the southern Otter Highlands (at Y-Nunatak). Some additional data from Paleozoic sediments of the northern Otter Highlands and the Haskard Highlands are also discussed.

The fieldwork was carried out by G. Kleinschmidt und W. Buggisch. About 300 samples were collected. In order to assess the degree of low grade metamorphism about 200 thin sections were studied with respect to the behaviour of quartz (i.e. pressure solution, deformation lamellae, grain boundary migration, formation of subgrains and recrystallization) as well as the growth of newly formed mica minerals. The microscopic investigations were supplemented by XRD studies (mainly illite crystallinity = IC) carried out by S. Krumm. K-Ar dates were determined on selected grain-size fractions of several samples at the Bundesanstalt für Geowissenschaften und Rohstoffe (BGR).

2. SAMPLE PREPARATION AND MEASUREMENT CONDITIONS

Detailed descriptions of the sample preparation methods are given in VON GOOSEN et al. (1991), BUGGISCH et al. (1990) and KRUMM & BUGGISCH (1991). Only a brief summary of important differences to other laboratories or to the recommendations of the IGCP illite crystallinity working group (KITSCH 1990, 1991) will be presented here.

Grain-size separation of the < 0.2 µm, 0.2-0.6 µm or < 0.6 µm (spherical equivalent diameters) fractions were carried out using a pipette centrifuge. Coarser fractions (0.6-2 µm, 2-6 µm, 6-20 µm and 20-63 µm) were separated by repeated settling in Atterberg tubes. For general investigations of IC, only the < 2 µm fraction was separated. Care was taken to repeat the settling several times. Otherwise, smaller grains are preferentially enriched in comparison to the limiting equivalent diameter.

For the determination of IC thin sedimentation slides (0.25 mg/cm²) with a high degree of orientation of the individual clay particles were produced. These extremely thin slides give higher intensities and narrower peak widths which seems to be in

* Prof. Dr. Werner Buggisch, Dr. Stefan Krumm, Geologisches Institut der Universität Erlangen, Schloßgarten 5, D-91054 Erlangen.
† Prof. Dr. Georg Kleinschmidt, Geologisch-Paläontologisches Institut der Universität Frankfurt, Senckenberganlage 32, D-60325 Frankfurt/Main.
‡ Dr. Hans Kreuzer, Bundesanstalt für Geowissenschaften und Rohstoffe, Stilleweg 2, Postfach 510153, W-3000 Hannover 51.

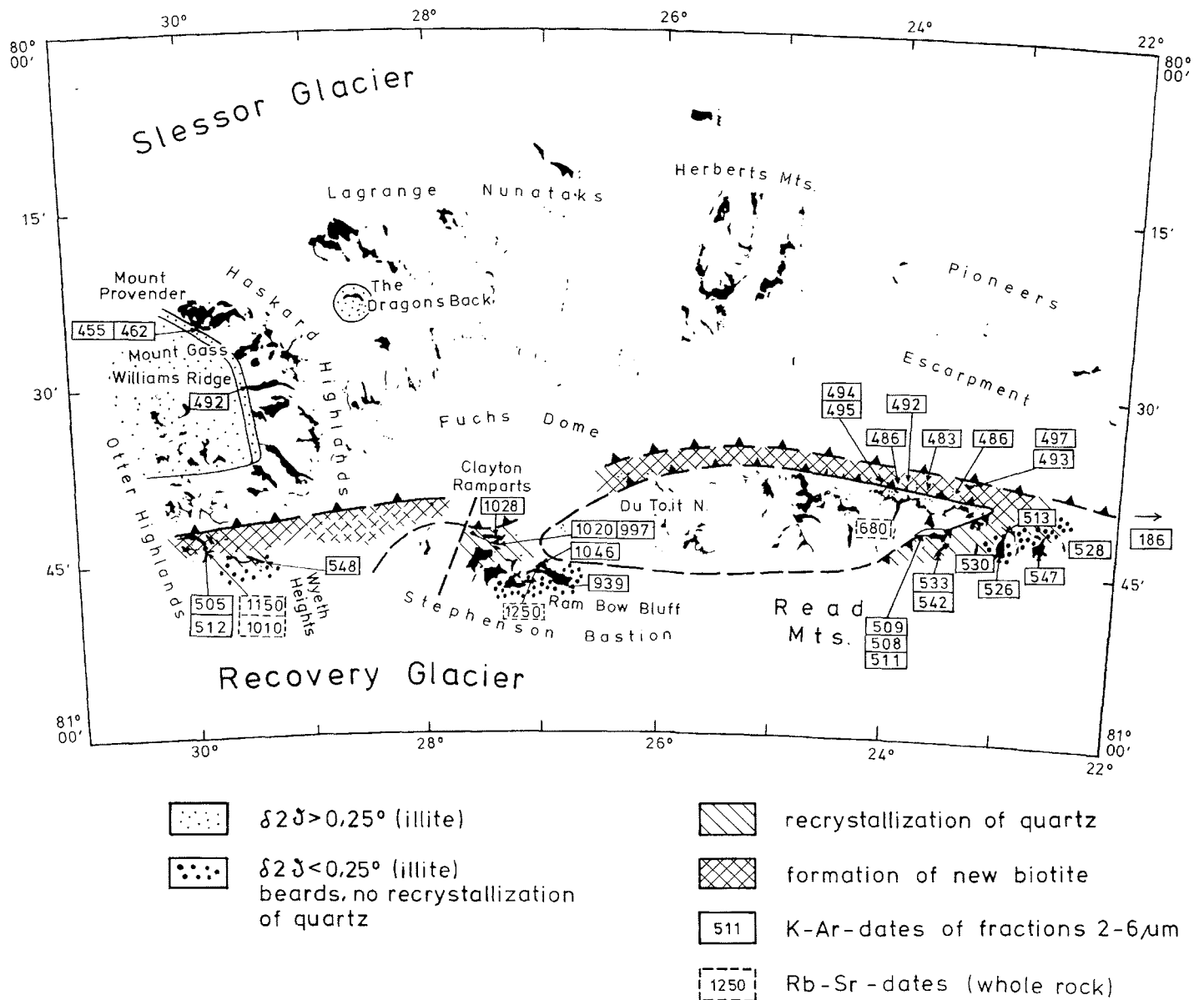


Fig. 1: Map of low-grade to very low-grade metasediments in the Shackleton Range with K-Ar and Rb-Sr dates.

Abb. 1: Verteilung der niedrigst- bis niedrig-gradigen metamorphen Sedimente in der Shackleton Range mit K-Ar- und Rb-Sr-Daten.

better accordance with metamorphic grade (at least if samples from very low grade to low grade areas are used) than conventionally used thicker slides (BUGGISCH 1986, KRUMM & BUGGISCH 1991).

2.1. Measurement conditions for IC

The measurements were controlled and evaluated by a computer. For describing „IC“ we prefer using the integral breadth instead of the KUBLER-index (half-height width). Line broadening due to small crystallite size and size distributions, which represents the physical meaning of „IC“, is more pronounced at the tails of the reflections (KLUG & ALEXANDER 1974). The half-height width is not as sensitive to this kind of broadening as the integral breadth. Due to this other peak breadth param-

ter and due to the extremely thin slides used, our „IC“ values cannot directly be compared to the KUBLER scale or attributed to the terms „anchi-“ and „epizone“. A first approximation is given by regression analysis from a plot of half-height width against integral breadth (KRUMM 1992).

The conventional limiting values for the anchizone and epizone boundaries correspond to the measurement conditions KUBLER used in his early work. These values are obtained with very high scanning speed and a large time constant (2-8° 2 θ /min, TC 2-4 sec). Therefore, the half-height width of 0.42 Δ° 2 θ and 0.25 Δ° 2 θ are too high for the measurement conditions we used (0.6 Δ° 2 θ /min, time constant 1 sec). KISCH (1990, 1991) calibrated his equipment against KUBLER's standards and found half-height values of 0.38 Δ° 2 θ for the diagenesis/anchizone transition and 0.21 Δ° 2 θ for the onset of low grade metamorphism. Because

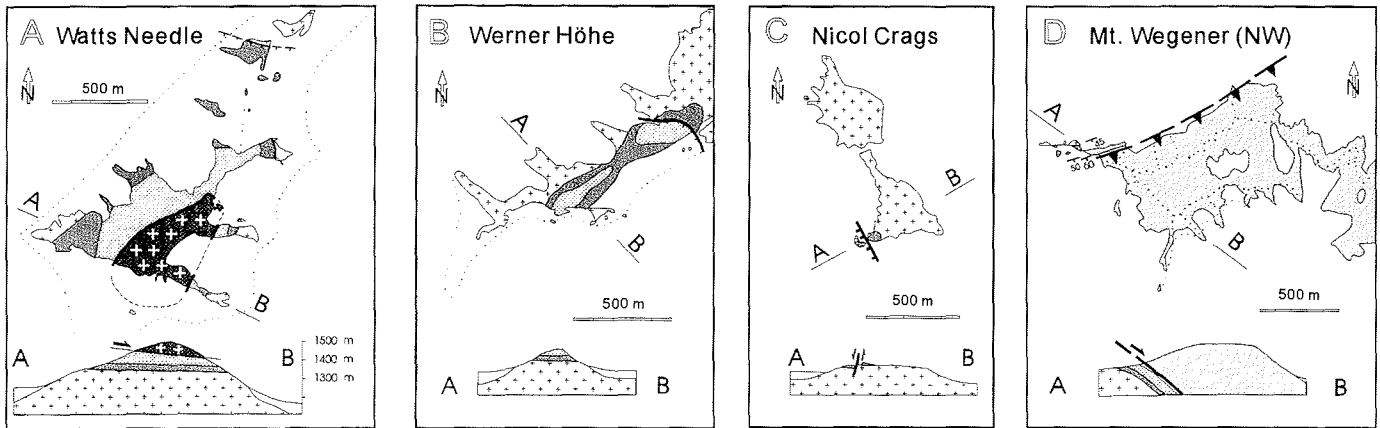
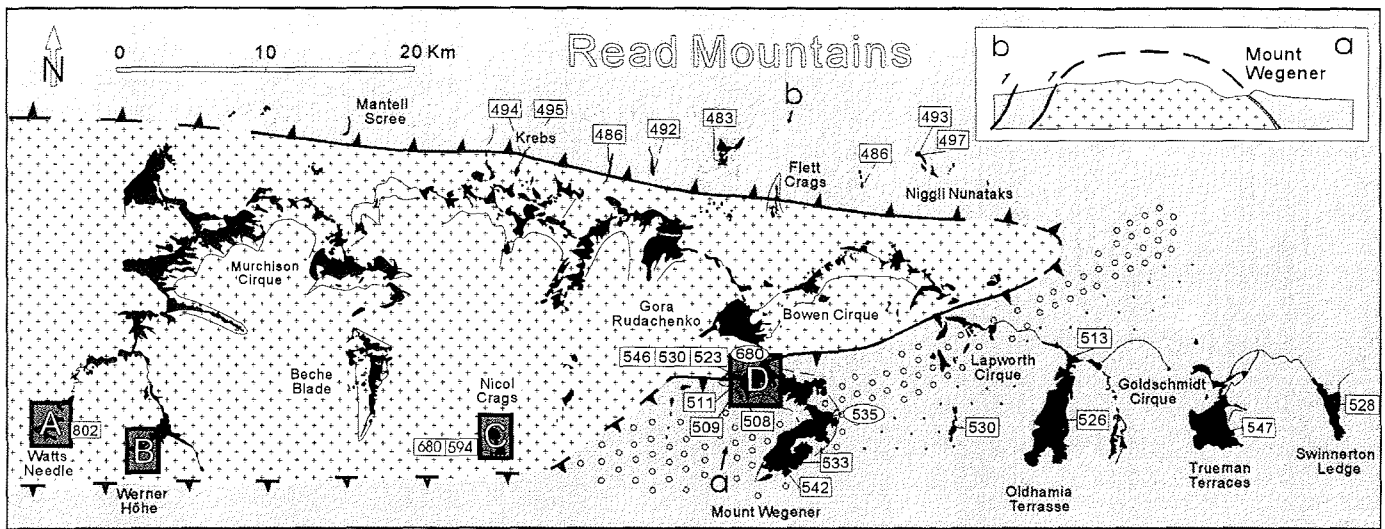


Fig. 2: Map of low-grade to very low-grade metasediments in the Read Mountains with K-Ar and Rb-Sr dates (top) and illite crystallinities of selected sections (left).

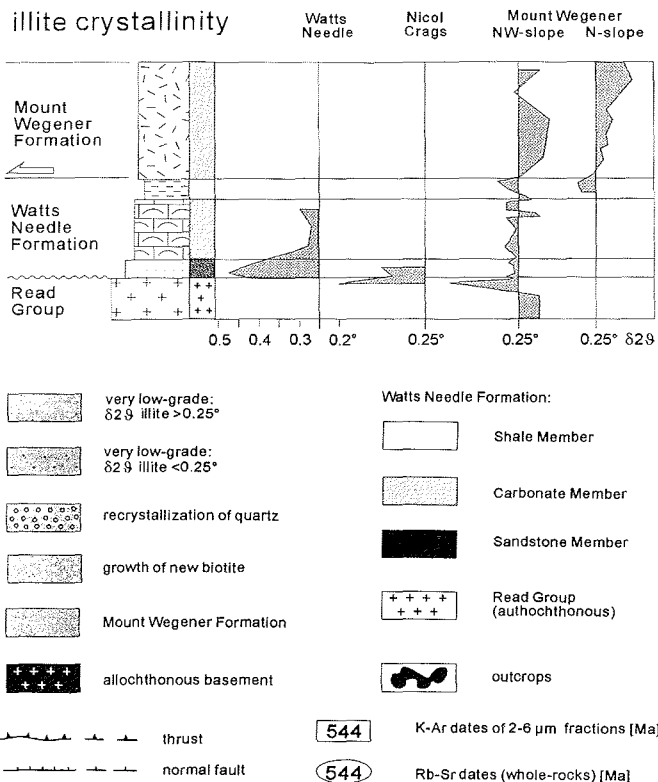


Abb. 2: Verteilung der niedrigst- bis niedrig-gradig metamorphen Sedimenten in den Read Mountains mit K-Ar- und Rb-Sr-Daten (oben) und Illit-Kristallinitäten ausgesuchter Profile (links).

scans of mica single crystals in our laboratory show the same diffractometer resolution as obtained on Kisch's equipment (KISCH 1990, $0.08 \Delta^2\theta$), we adopted those values for the characterization of metamorphic grade. The lower limit of the anchizone then corresponds to an integral breadth of $0.57 \Delta^2\theta$, its upper limit to $0.34 \Delta^2\theta$ respectively for conventionally thick slides. However, it can be shown (KRUMM & BUGGISCH 1991) that (very) thick specimens have a strong grain-size gradation and poor particle orientation. Therefore, small grains with low crystallinity are preferentially measured, larger particles are excluded. If thin specimens are used, each particle has the same opportunity to contribute to diffraction. For this reasons, thin slides generally show narrower breadths than thicker ones (see also JABOYEDOFF & THELIN 1990).

Considering the statistical nature of „IC“, it seems that the influence of the thin specimens is offset by effects from using integral breadth. Therefore it is reasonable to adopt Kisch's half-height width values also for our measurement conditions (thin slides but integral breadth) as a first approximation. More re-

liable correlations will be possible from the results of several inter-laboratory studies currently being carried out. In order to enable a later recalculation of the IC values used in this work, we document the integral breadths measured on the „Crystallinity Index Standards“ (CIS) of WARR & RICE (1994): SW1 = $0,76 \Delta^\circ 2\vartheta$, SW2 = $0,48 \Delta^\circ 2\vartheta$, SW4 = $0,36 \Delta^\circ 2\vartheta$, SW6 = $0,21 \Delta^\circ 2\vartheta$.

In general, decreasing sizes of analysed grain fractions result in broadening of illite peaks. Plots of „IC“ and „crystallinity“ of chlorite versus grain size exhibit two patterns (Fig. 3). Samples from the frame of the Read Window (e.g. Mount Wegener Formation) show more or less the same crystallinities in fractions from 60 μm down to 0.6 μm . A pronounced decrease of both „IC“ and chlorite „crystallinity“ is observed toward smaller size fractions.

This decrease below the 0.6 μm grain size limit is documented in samples from Stephenson Bastion and Wyeth Heights, as well. However, in contrast to the samples from the Mount Wege-

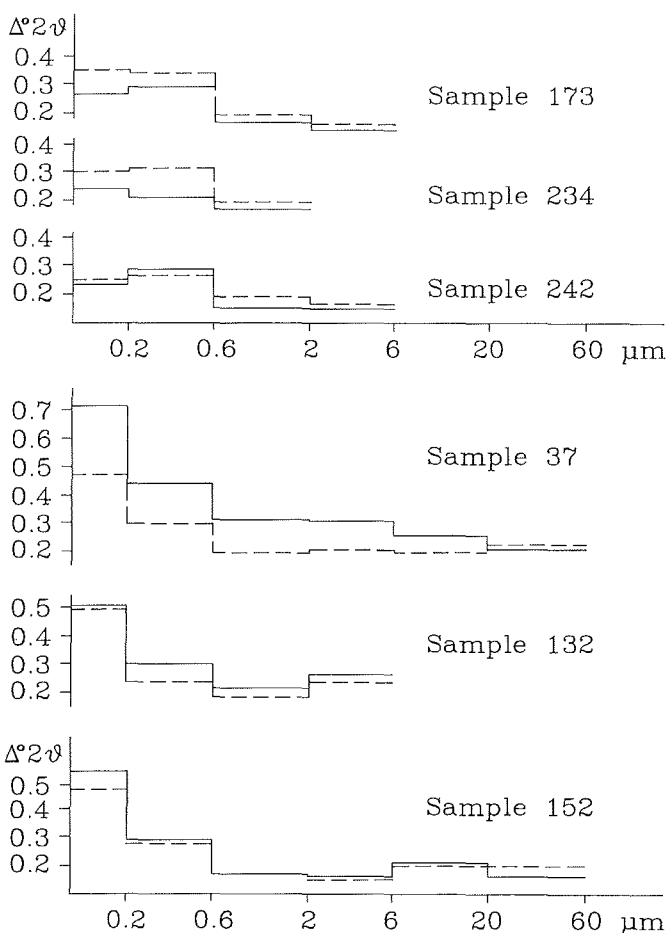


Fig. 3: Relationship between illite (= solid line) and chlorite (= dashed line) crystallinities and grain-size dependent on localities; 37 = Niggli Nunatak, 132 = Mount Wegener S, 152 = Mount Wegener N, 173 = Wyeth Heights, 234 = Ram Bow Bluff, 242 = Clayton Ramparts.

Abb. 3: Beziehung zwischen Illit- und Chlorit-Kristallinität (Chlorit gestrichelt) und Korngröße. Lokalitäten: 37 = Niggli Nunatak, 132 = Mount Wegener S, 152 = Mount Wegener N, 173 = Wyeth Heights, 234 = Rambow Bluff, 242 = Clayton Ramparts.

ner Formation no further decrease occurs in the $< 0.2 \mu\text{m}$ fraction. Therefore, we might speculate that two different populations of (clay minerals and/or) mica occur at Stephenson Bastion and Wyeth Heights.

In general the question arises: do the size fractions represent a primary grain-size distribution or are they completely an artifact of sample preparation? Obviously the amount of fine-grained fraction ($< 2 \mu\text{m}$ and $0.2-0.6 \mu\text{m}$) produced during our preparation increases with decreasing metamorphic degree of the sample. Therefore, the grain-size distribution is related to the geological history of the sample. Taking into account a diameter/thickness ratio between 10:1 and 20:1 (MERRIMAN et al. 1990) for the phyllosilicates in the analyzed fraction the observed change in IC and chlorite „crystallinity“ might be due to particle thickness. Further investigations are in progress and will be published later.

2.2. K-Ar-dating

Grain-size fractions from shales and schists (see sample preparation) were used for conventional K-Ar analyses. All samples or fractions were examined in thin sections, by XRD and some by SEM. The methods are described in BUGGISCH et al. (1990). K was determined by flame photometry, Ar by conventional total fusion static massspectrometric isotope dilution analysis (SEIDEL et al. 1982). The IUGS-recommended constants (STEIGER & JÄGER 1977) were used. Our K-Ar date on the interlaboratory standard glaucony GL-O is 1% younger than the mean value of the compilation of ODIN (1982).

Any interpretation of the K-Ar dates (Tab. 2, Figs. 1 and 2) is open to criticism due to the uncertainty to what extent Ar is preserved in detrital or early formed mica or is lost by later processes.

A dependence of K-Ar dates on measured grain-sizes and illite crystallinity is observed (Fig. 4). The values of all of these parameters depend on the geological history of the samples, but are subject to sample preparation and measurement conditions as well. Radiogenic argon and „illite crystallinities“ can be inherited if the rocks are not completely overprinted during diagenesis or metamorphism. Most authors agree that detrital components - if present - are enriched in the coarse grains whereas authigenic minerals are enriched in the fine-grained size fractions. Therefore, examination of different size fractions should enable to distinguish between inherited (detrital) and acquired (diagenetic or metamorphic) ages and „crystallinities“ (further discussion see REUTER 1985: 6 ff.). But this assumption is obviously too simple for the interpretation of our data.

In our material, the phyllosilicates of all samples consist exclusively of illite/sericite, chlorite and biotite. In addition, quartz is present in the coarser fractions. Paragonite and pyrophyllite are not observed in samples used for K/Ar dating. The ratio of chlorite to sericite (+biotite) was estimated from the integration of (001) peaks of illite+sericite+biotite and (002) of chlorite.

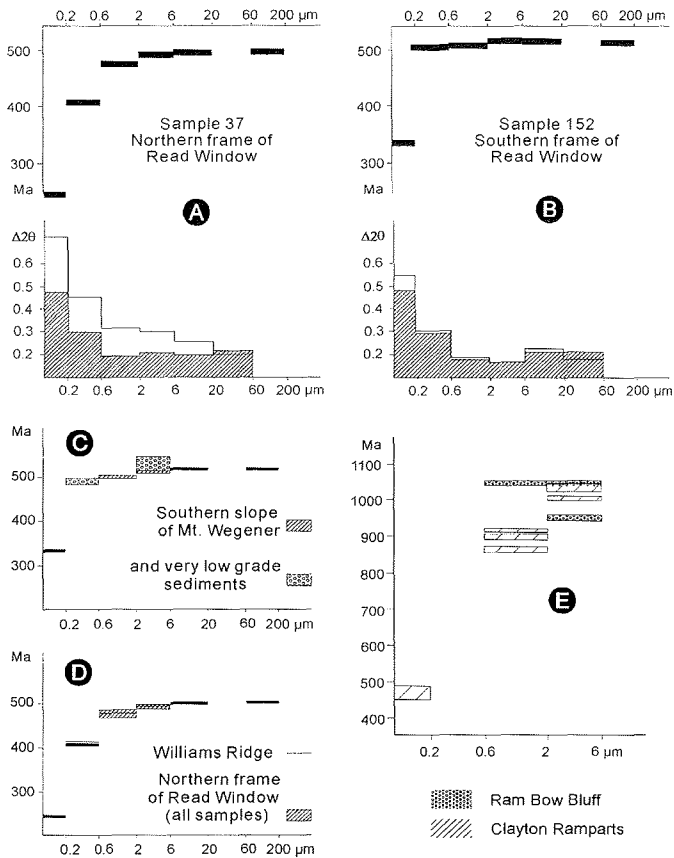


Fig. 4: K-Ar dates versus grain-size: (A and B) on two selected samples from the Read Mountains compared with the crystallinity of illite (and chlorite = hatched) $[\Delta 2\delta]$ versus grain size $[\mu\text{m}]$; (C) on samples from Mount Wegener, Oldhamia Terrace, Trueman Terraces and Swinnerton Ledge; (D) from the northern Read Mountains and Williams Ridge; (E) from Stephenson Bastion.

Abb. 4: K-Ar-Daten versus Korngröße zweier ausgewählter Proben der Read Mountains (A und B) im Vergleich mit der Illit- (Chlorit = schraffiert) Kristallinität $[\Delta 2\delta]$ versus Korngröße $[\mu\text{m}]$. (C) aus Proben von Mount Wegener, Oldhamia Terrasse, Trueman Terrasse und Swinnerton Ledge, (D) aus nördlichen Read Mountains und Williams Ridge, (E) von Stephenson Bastion.

Because the intensity of the reflection of both mineral groups depends very much on structure and composition, no effort was made to introduce corrections in order to gain semiquantitative data.

The grain-size fractions contain different amounts of chlorite, but no general trend or enrichment is observed. In contrast to BRAUCKMANN (1984), the „IC“ corresponds very well to the „crystallinity“ of chlorite (Fig. 3) in the different fractions (see FREY 1987).

The plots of „ICs“ and K-Ar dates versus grain-size (Fig. 4) exhibit more or less pronounced younging toward more fine-grained fractions. Therefore, similar questions to those for „IC“ arise: are the dates artifacts or do they trace any geological events [inherited age of source area of the sediments, diagenesis, peak of metamorphism or cooling age, retrograde alteration and/or new formation of mica, diffusion of Ar during cooling (HUNZIKER et al. 1986), loss of Ar due to preparation procedures (GERLING et al. 1963)]? HUNZIKER (1987) demonstrated that illites loose Ar also below the closing temperature assumed for high-temperature white micas. This effect depends on time, tem-

perature and grain-size. The K-Ar dates of $< 2 \mu\text{m}$ fractions are completely reset if they were at a temperature of $260 \text{ }^\circ\text{C}$ for about 10 Ma. A loss of about 50 % of Ar occurs already at $150 \text{ }^\circ\text{C}$ during the same time. Coarse-grained mineral fractions are less influenced and might preserve an older geological event (for instance, the time of mineral formation or of post-metamorphic cooling below the closure temperature). Detrital mica is enriched in the coarse-grained fractions. On the other hand, minerals might be not completely disintegrated in the very coarse fractions which therefore do not represent real crystal sizes but grain aggregates. Hence, the K-Ar dates might be either older than diagenesis/metamorphism (detrital mica) or younger (due to very small phyllosilicates in the insufficiently disintegrated grains).

A younging of detrital mica and/or early diagenetic clay minerals is documented in the dates from the trilobite shales of the Haskard Highlands Formation at Mount Provender. On the basis of trilobites (SOLOVIEV & GRIKUROV 1979), the age of sedimentation is Middle Cambrian. But, in spite of the fact that neither cleavage formation nor the growth of new phyllosilicates is observed in thin sections, K-Ar dates of the 2-6 μm fraction are scattered about 455 and 465 Ma which give evidence for a later overprint of this formation which might coincide with the weak deformation of the trilobites (see BUGGISCH et al. 1994, Fig. 22).

To approximate the age of diagenesis or metamorphism in the southern Shackleton Range we have chosen the K-Ar dates of the 2-6 μm fraction as a compromise. Of course, any of the following interpretations are highly speculative.

3. EAST ANTARCTIC CRATON

3.1. Basement rocks of the Read Mountains (Read Window)

This paper is not focused on the medium to high grade metamorphic basement rocks (Read Group). Nevertheless, there are some important observations:

- (1) K-Ar analyses on biotites from the Read Group yielded dates between 1650 and 1400 Ma. These determinations are corroborated by Rb/Sr dates within the same range (see Appendix, see also PANKHURST et al. 1983, REX 1972, HOFMANN et al. 1980).
- (2) Late granitic intrusions within the Read Group were not penetratively deformed during later events. Rather, later deformation known at the base of and within the hanging Mount Wegener Nappe is concentrated in discrete shear zones. Hence, the basement rocks of the Read Mountains (Read Group) were not affected by any regional metamorphism related to the Ross Orogeny.

3.2. The sedimentary cover of the Read Group

The unconformable sedimentary contact of the Read Group and the overlying Watts Needle Formation is exposed in four out-

Locality	Sample No. rock type		Rb ^{a)} (ppm)	Sr ^{a)} (ppm)	⁸⁷ Rb/ ⁸⁶ Sr ^{b)}	⁸⁷ Sr/ ⁸⁶ Sr ^{b)}	biotite-Wr ^{c)} isochron dates
Strachey Stump 23° 10.5' W 80° 40.1' S	HR 003 amphibolite layer	WR bi	88.1 409	374 16	0.6815 82.56	0.71727 2.4648	1487 ± 30 Ma IR 0.7027 ± 6
	HR 001 granodioritic gneisses	WR	83.0	121	1.999	0.74374	
	HR 002	WR	116	299	1.130	0.73257	
Mount Wegener 23° 36.0' W 80° 42.0' S	W 138 granite	WR	161	39.8	12.053	1.00108	
W of Mount Wegener 23° 46.3' W 80° 43.0' S	W 127 monzonite	WR bi	138 432	1786 86.1	0.224 15.00	0.71067 1.05058	1602 ± 33 Ma IR 0.7055 ± 5
Nicol Craigs 24° 05.0' W 80° 43.8' S	HR 005 HR 006 HR 007 aplitic granites	WR WR WR	196 185 162	199 191 222	2.869 2.812 2.120	0.77633 0.77489 0.76851	
Beche Blade 24° 20.8' W 80° 42.0' S	HR 148 diorite HR 147 granitic vein	WR bi WR	73.8 351 110	922 28.3 512	0.2319 39.00 0.6251	0.71139 1.56322 0.72298	1531 ± 31 Ma IR 0.7063 ± 5
Pt. 1246, ridge SE of The Arc, E of Watts Needle 24° 38.9' W 80° 44.3' S	HR 195 qtz. monzodiorite HR 198 monzodiorite	WR bi WR bi	91.0 361 83.8 297	1070 36.7 1325 76.5	0.2464 30.43 0.1830 11.53	0.71143 1.38550 0.70994 0.96736	1555 ± 31 Ma IR 0.7059 ± 5 1580 ± 32 Ma IR 0.7058 ± 4
SW of Kuno Cirque 25° 04.2' W 80° 40.9' S	HR 079 granitic vein	WR	159	127	3.662	0.79596	

Tab. 1: Rb-Sr data of Read Group rocks, basement of the Read Window (A. HÖHNDORF, P. MÜLLER, N. ROLAND). ^{a)} Rb, Sr concentrations in ppm, NBS 987 = 0.71023 ± 0.00007; analytical precision at the level of 95 % confidence: $d(^{87}\text{Rb}/^{86}\text{Sr}) = 2\%$, $d(^{87}\text{Sr}/^{86}\text{Sr}) = 0.06\%$. ^{b)} Normalized to $^{86}\text{Sr}/^{88}\text{Sr} = 0.1194$. ^{c)} IUGS-recommended constants (STEIGER & JÄGER 1975); errors are quoted at the level of 95 % confidence and refer to the last digit(s). Abbreviations: bi = biotite, IR = initial ration, WR = whole rock.

Tab. 1: Rb-Sr-Daten von Gesteinen der Read-Gruppe; Unterlage des Read-Fensters.

crops: (1) Watts Needle (Fig. 7), (2) Werner Nunatak, (3) Nicol Craigs (Fig. 6), and (4) northwest corner of Mount Wegener (Fig. 5). The Late Precambrian weathering of the Read Group produced a smooth relief covered by a palaeosoil (PAECH et al. 1987). At all localities mentioned above, this rheolith is preserved in pockets and depressions at the base of the Sandstone Member of the Watts Needle Formation and reaches a thickness of more than two metres at Nicol Craigs (Fig. 6). The soil at some localities is completely undeformed and still almost unlithified forming a typical „grus“. According to the broad (001)-peaks (integral breadth between 0.4 to 0.5 $\Delta^\circ 2\theta$, Fig. 2) the crystallinity of illite and chlorite is close to the boundary between diagenesis and anchimetamorphism (= very low grade metamorphism). This is corroborated by the occurrence of kaolinite in the palaeosoil at Nicol Craigs.

The coexistence of kaolinite and pyrophyllite in some samples at the base of the Sandstone Member allows an estimation of the metamorphic conditions. According to the reaction kaolinite + quartz \rightarrow pyrophyllite + H₂O the system is univariant at fixed water activities. „Under the condition, that water pressure equals lithostatic pressure ($a_{\text{H}_2\text{O}} = 1$)“ the transformation temperature is 300 °C at 2 kbar and 310 at 5 kbar“ (FREY 1987 a).

Assuming activities of H₂O between 0.8 and 1.0 the stability limits range from 250 to 310 °C. FREY (1987b) estimated by coal rank and fluid inclusion data the following conditions for kaolinite and pyrophyllite bearing metaclastites of the external zone of the Swiss Alps: 2-3 kbar, 270 °C, and $a_{\text{H}_2\text{O}}$ of about 0.7. The low water activity may be due to the generation of CO₂ from CaCO₃. These values might be close to the conditions in our

Location rock type	Sample No	mineral	fraction (μm)	K-Ar Date (Ma)	K (wt.%)	$^{40}\text{Ar}_{\text{rad}}$ (nl/g STP)	$^{40}\text{Ar}_{\text{atm}}$
-----------------------	--------------	---------	-------------------------------	-------------------	-------------	---	-------------------------------

Read Group

Basement rocks of the Read Window (H. KREUZER, P. MÜLLER, N. ROLAND)

Strachey Stump biotite amphibolite layer	HR 003	bi	100-250	1420 ± 9	7.21 (4)	605 (3)	1.6 (5)
		bi	50-100	1338 ± 7	7.08 (4)	545 (3)	1.6 (8)
W of Mount Wegener monzonite	W 127	hb+bi	125-200	1584 ± 23	1.552 (31)	153.0 (12)	1.1 (4)
		hb+bi	63-125	1659 ± 23	1.294 (26)	136.9 (11)	0.8 (4)
		bi	250-400	1617 ± 11	7.17 (6)	730 (6)	2.3 (6)
		bi	200-250	1619 ± 11	7.11 (6)	725 (6)	2.4 (10)
Beche Blade	HR 148	hb	125-200	1603 ± 16	0.867 (17)	87.0 (7)	1.0 (1)
		hb	63-125	1672 ± 16	0.816 (16)	87.3 (7)	0.8 (1)
		bi	315-500	1546 ± 11	7.14 (6)	679 (5)	2.9 (5)
		bi	250-315	1544 ± 11	6.81 (5)	646 (5)	1.9 (9)
Pt. 1246 ridge SE of The Arc E of Watts Needle quartz monzodiorite	HR 195	hb+bi	125-200	1548 ± 22	1.168 (23)	111.3 (9)	0.5 (3)
		hb+bi	63-125	1661 ± 23	0.864 (17)	91.5 (7)	0.8 (3)
		bi	250-400	1645 ± 12	6.97 (5)	728 (6)	2.0 (6)
		bi	200-250	1630 ± 12	6.74 (5)	694 (5)	2.1 (9)
monzodiorite	HR 198	hb+bi	125-200	1528 ± 22	1.177 (24)	110.0 (9)	0.9 (3)
		hb+bi	63-125	1588 ± 23	1.008 (20)	99.8 (8)	2.9 (3)
		bi	250-300	1608 ± 25	6.70 (9)	676 (15)	2.1 (6)
		bi	200-250	1590 ± 22	6.68 (4)	662 (13)	1.6 (9)

Watts Needle Formation - sedimentary cover of the Read Group (basal member, increasing deformation from Watts Needle to Mount Wegener)

E ridge Watts Needle slate	1	TR	2-6	802 ± 7	3.21 (3)	126.0 (10)	0.7 (2)
		TR	0.6-2	714 ± 7	2.90 (2)	98.6 (8)	1.1 (2)
		TR	<0.6	389 ± 4	2.25 (2)	37.9 (3)	1.7 (1)
Nicol Crag quartzwacke	33	TR	2-6	594 ± 6	5.57 (4)	152.3 (12)	1.4 (4)
		TR	0.6-2	601 ± 6	6.78 (5)	187.9 (14)	0.8 (3)
		TR	<0.2	529 ± 5	7.12 (6)	170.2 (13)	0.8 (3)
Nicol Crag red slate	32	TR	2-6	680 ± 6	4.78 (4)	153.7 (12)	0.6 (2)
		TR	0.6-2	612 ± 6	5.68 (5)	161.0 (12)	0.8 (3)
		TR	0.6	521 ± 5	5.86 (5)	137.5 (11)	0.9 (3)
WNW tip Mt. Wegener basal quartzwacke	57	TR	2-6	530 ± 5	4.70 (4)	112.6 (9)	1.7 (2)
		TR	0.6-2	511 ± 5	6.50 (5)	149.2 (11)	0.8 (3)
		TR	<0.6	481 ± 5	6.67 (5)	142.9 (11)	1.3 (2)
WNW tip Mt. Wegener quartzwacke	50	TR	2-6	523 ± 5	4.92 (4)	115.9 (9)	0.6 (2)
		TR	0.6-2	512 ± 5	6.67 (5)	153.6 (12)	0.6 (3)
		TR	<0.6	480 ± 5	7.17 (6)	153.2 (12)	1.0 (3)
WNW tip Mt. Wegener siltstone	51b	TR	2-6	546 ± 5	7.15 (6)	177.2 (14)	0.5 (3)
		TR	0.6-2	556 ± 5	6.97 (5)	176.2 (13)	0.7 (3)
		TR	<0.6	485 ± 5	7.20 (6)	155.8 (12)	0.5 (3)

Location rock type	Sample No	mineral	fraction (μm)	K-Ar Date (Ma)	K (wt.%)	$^{40}\text{Ar}_{\text{rad}}$ (nl/g STP)	$^{40}\text{Ar}_{\text{atm}}$
Metasedimentary Mount Wegener Nappe, Mount Wegener Formation; Northern Read Mountains, biotite zone							
Niggli Nunatak (N) biotite schist	36	TR	2-6	493 ± 5	4.77 (3)	104.9 (8)	0.1 (2)
		TR	0.6-2	475 ± 4	4.75 (3)	100.2 (8)	0.2 (1)
Niggli Nunatak (N) biotite schist	37	TR	63-200	500 ± 5	3.23 (3)	72.2 (5)	0.4 (1)
		TR	6-20	498 ± 5	3.00 (2)	66.7 (5)	0.3 (1)
		TR	2-6	497 ± 3	3.74 (2)	83.2 (4)	0.4 (1)
		TR	0.6-2	479 ± 7	3.87 (3)	82.4 (11)	0.3 (1)
		TR	0.2-0.6	410 ± 4	4.49 (3)	80.4 (4)	0.6 (1)
		TR	<0.2	244 ± 3	6.52 (5)	66.2 (8)	2.0 (1)
W of Niggli Nunatak (2) biotite schist	38	TR	2-6	486 ± 5	4.10 (3)	88.9 (7)	0.5 (1)
		TR	0.6-2	467 ± 5	3.89 (3)	80.6 (6)	1.2 (2)
Nunatak (5) biotite schist	45	TR	2-6	483 ± 5	5.48 (4)	117.9 (9)	0.4 (2)
		TR	0.6-2	470 ± 5	5.19 (4)	108.1 (8)	0.4 (2)
Nunatak (6) biotite schist	47	TR	2-6	492 ± 5	2.98 (2)	65.5 (5)	0.2 (1)
		TR	0.6-2	477 ± 5	3.39 (2)	71.9 (5)	0.5 (1)
Nunatak (10) biotite schist	88b	TR	2-6	486 ± 5	5.24 (4)	113.8 (9)	0.1 (1)
		TR	0.6-2	468 ± 5	5.27 (4)	109.5 (8)	0.5 (2)
Nunatak (11) biotite schist	90	TR	2-6	494 ± 5	5.20 (3)	114.9 (9)	0.1 (1)
		TR	0.6-2	475 ± 5	4.62 (4)	97.7 (7)	0.2 (2)
Nunatak (11) mylonite	96	TR	2-6	495 ± 5	6.01 (4)	133.0 (10)	0.5 (2)
		TR	0.6-2	483 ± 5	5.90 (4)	126.9 (10)	0.7 (2)
Southern Read Mountains, shales with subordinate biotite							
NW tip of Mount Wegener	155	TR	2-6	509 ± 5	3.37 (2)	77.1 (6)	0.2 (1)
			0.6-2	495 ± 5	4.94 (3)	109.2 (8)	0.2 (2)
NW tip of Mount Wegener	156	TR	2-6	511 ± 5	4.26 (3)	97.8 (7)	0.3 (1)
			0.6-2	500 ± 5	5.40 (4)	121.0 (9)	0.4 (1)
NW tip of Mount Wegener	152	TR	200-630	514 ± 5	3.54 (3)	81.7 (6)	0.5 (1)
			63-200	517 ± 5	3.44 (3)	80.2 (6)	0.3 (1)
			6-20	517 ± 5	3.13 (3)	72.8 (6)	0.2 (1)
			2-6	508 ± 4	3.45 (2)	79.0 (6)	0.1 (2)
			0.6-2	501 ± 5	5.09 (4)	114.1 (9)	0.0 (2)
			<0.2	333 ± 3	6.06 (4)	86.1 (7)	0.6 (2)
Southern Read Mountains, shales still with recrystallization of quartz							
S slope of Mount Wegener	132	TR	2-6	542 ± 4	3.62 (2)	88.5 (5)	0.3 (4)
			0.6-2	515 ± 5	4.90 (5)	113.5 (9)	0.4 (2)
			<0.2	339 ± 3	6.14 (5)	88.8 (7)	0.9 (2)
S slope of Mount Wegener	136	TR	2-6	533 ± 3	3.53 (2)	85.2 (4)	0.3 (1)
			0.6-2	511 ± 4	4.86 (4)	111.8 (6)	0.3 (1)
			<0.2	426 ± 4	4.75 (4)	88.6 (4)	0.5 (1)

Location rock type	Sample No	mineral	fraction (μm)	K-Ar Date (Ma)	K (wt.%)		$^{40}\text{Ar}_{\text{rad}}$ (nl/g STP)	$^{40}\text{Ar}_{\text{atm}}$
Southern Read Mountains, very low grade shales (<0.25) °2 δ illite								
	105	TR	2-6	530 \pm 5	3.93	(3)	93.7 (7)	0.7 (1)
		TR	<0.6	476 \pm 5	6.22	(5)	131.8 (10)	0.7 (2)
	129	TR	2-6	513 \pm 5	3.86	(3)	89.1 (7)	0.2 (1)
		TR	<0.6	497 \pm 5	5.14	(4)	114.3 (9)	1.0 (2)
Southern Read Mountains, very low grade shales (>0.25) °2 δ illite								
Oldhamia Terrasses	124	TR	2-6	526 \pm 5	3.44	(3)	81.6 (6)	0.5 (1)
		TR	<0.6	480 \pm 5	5.91	(5)	126.3 (10)	0.6 (2)
Trueman Terrasses	119	TR	2-6	547 \pm 5	3.21	(3)	79.8 (6)	0.3 (1)
		TR	<0.6	497 \pm 5	5.87	(5)	130.5 (10)	0.6 (2)
Swinnerton Ledge	112	TR	2-6	528 \pm 5	4.22	(3)	100.7 (8)	0.4 (1)
		TR	<0.6	483 \pm 5	6.59	(3)	1417 (7)	0.5 (2)
Wyeth Heights Formation - metasedimentary Mount Wegener Nappe of the Otter Highlands, biotite schists, close to the northern nappe boundary								
south of camp	168	TR	2-6	512 \pm 5	7.01	(6)	161.2 (12)	0.4 (2)
		TR	0.6-2	498 \pm 5	6.48	(5)	144.4 (11)	0.8 (1)
south of camp	169	TR	2-6	505 \pm 11	6.08	(3)	137.7 (32)	1.0 (2)
		TR	0.6-2	492 \pm 7	5.56	(4)	122.2 (16)	0.9 (2)
		TR	<0.2	267 \pm 3	6.02	(5)	67.3 (5)	0.8 (2)
near Wyeth Heights	173	TR	2-6	548 \pm 5	5.30		231.1 (7)	0.8 (1)
		TR	0.6-2	515 \pm 5	5.68	(5)	131.6 (10)	0.9 (1)
		TR	0.2-0.6	484 \pm 5	5.26	(4)	113.3 (9)	3.7 (7)
		TR	<0.2	304 \pm 3	6.12	(5)	78.7 (7)	5.5 (7)
Stephenson Bastion Formation - basal (?) part of metasedimentary Mount Wegener Nappe, originally regarded as Mount Wegener Formation for structural reasons								
southwest of Clayton Ramparts, shale	234	TR	2-6	1020 \pm 9	3.40	(3)	181.2 (14)	0.5 (3)
		TR	0.6-2	904 \pm 8	3.67	(3)	167.4 (13)	0.6 (2)
		TR	<0.2	486 \pm 5	4.98	(4)	108.0 (8)	0.5 (2)
southwest of Clayton Ramparts, shale	235	TR	2-6	997 \pm 8	5.18	(4)	267.7 (20)	0.5 (3)
		TR	0.6-2	855 \pm 7	5.32	(4)	226.2 (17)	0.2 (2)
Clayton Ramparts shale	242	TR	2-6*	1028 \pm 9	3.75	(3)	201.7 (15)	0.2 (2)
		TR	0.6-2	882 \pm 8	3.78	(3)	167.3 (13)	0.7 (1)
		TR	<0.2	452 \pm 5	4.18	(3)	83.3 (8)	1.3 (5)
				* see also Ar-Ar spectrum				
Ram Bow Bluff siltstone	226	TR	2-6	939 \pm 7	3.024	(22)	144.8 (8)	0.5 (2)
		TR	0.6-2	1036 \pm 7	4.458	(10)	242.6 (20)	0.8 (2)
Ram Bow Bluff siltstone	244	TR	2-6	1046 \pm 8	2.063	(17)	113.6 (9)	0.3 (2)
		TR	0.6-2	1045 \pm 9	3.70	(3)	203.8 (15)	0.7 (2)

Location rock type	Sample No	mineral	fraction (μm)	K-Ar Date (Ma)	K (wt.%)	$^{40}\text{Ar}_{\text{rad}}$ (nl/g STP)	$^{40}\text{Ar}_{\text{atm}}$
Pioneers Group							
Williams Ridge Formation							
Williams Ridge mica schist	212	TR	2-6	492 ± 4	4.53 (4)	99.6 (6)	0.3 (1)
		TR	0.6-2	478 ± 6	4.68 (4)	99.6 (11)	0.2 (1)
		TR	<0.6	418 ± 6	4.66 (4)	85.2 (12)	0.5 (1)
Haskard Highlands Formation, weakly tectonized Middle Cambrian trilobite shales							
Moraine SSW of Mount Provender	183e	TR	2-6	455 ± 5	2.439 (20)	49.0 (4)	0.8 (1)
		TR	0.6-2	451 ± 5	3.170 (26)	63.1 (5)	0.8 (1)
		TR	<0.6	422 ± 4	4.81 (4)	88.9 (7)	0.7 (2)
Moraine SSW of Mount Provender	183g	TR	2-6	462 ± 5	2.506 (21)	51.3 (4)	0.5 (1)
		TR	0.6-2	448 ± 5	3.281 (27)	64.8 (5)	0.5 (1)
		TR	<0.6	424 ± 4	5.30 (4)	98.5 (8)	0.7 (2)
Volcanogenic rock approx. 50 km east of Read Mountains							
	148	TR	2-6	186.3 ± 2.0	2.667 (22)	20.33 (16)	0.5 (1)
		TR	0.6-2	180.6 ± 1.9	4.427 (35)	32.68 (25)	0.3 (1)

Tab. 2: K-Ar-data. Argon in nanoliter per gram at standard pressure and temperature, corrected for mean values of blank analyses. IUGS-recommended constants (STEIGER & JÄGER 1977) are used. Our date for standard glauconite GL-O is 1 % younger than the average value of the compilation of ODIN (1982). Error estimates are quoted at a level of 95 % confidence of intralaboratory analytical precision. Those in parentheses refer to the last digit(s). For hornblendes contaminated by biotite the relative error of the K determination is arbitrarily increased by 2 % in order to account for possible inhomogeneities. Abbreviations: bi = biotite, hb = hornblende, TR = size fraction of whole-rock.

Tab. 2: K-Ar-Daten. Ar in Nanoliter per Gramm bei Normaldruck und Temperatur.

material from the Watts Needle Formation.

According to the age estimates from Rb-Sr whole rock analyses of PANKHURST et al. (1983) and BUGGISCH et al. (1994) the age of sedimentation of the Sandstone Member is about 700 Ma. This is more or less in agreement with the fossil record (WEBER 1991). A K-Ar analysis of the 2-6 μm fraction from shales near the base of the Watts Needle section, which are least affected by Ross aged influence (Fig. 2) gave a date of about 800 Ma.

The sediments of the Sandstone Member of the Watts Needle Formation are not or only weakly deformed. At Nicol Crags detrital quartz is affected by weak pressure solution. The grains and their secondary overgrowth show only very slight undulatory extinction. The boundaries between different syntaxial quartz cements are often straight. No cleavage can be observed in the basal quartzwackes at Nicol Crags. At Mount Wegener a growing influence of metamorphism upwards is indicated by increasing pressure solution of quartz grains and incipient formation of chlorite (-quartz-illite) beards in the Sandstone Member. Deformation increases toward a major thrust plane, called the Mount Wegener Thrust (KLEINSCHMIDT et al. 1992). This

thrust plane cuts off the Watts Needle Formation at different levels. At Watts Needle, crystalline basement rocks are thrust over the Limestone Member. Here, limestones are strongly foliated, folded and recrystallized forming limestone mylonites (Fig. 7). At Mount Wegener the most complete section of the Watts Needle Formation is preserved. It is cut off within the Shale Member. The thrust plane is marked by meter-sized slabs of crystalline basement rocks (Fig. 8). The schistosity and metamorphism increases towards the hanging thrust plane in all sections. This is corroborated by improving illite crystallinity (Fig. 2).

There is no continuous sedimentary transition from the Watts Needle Formation to the Mount Wegener Formation as assumed by most of the authors (CLARKSON 1972, 1982b, 1983; PAECH 1986).

PAECH (1982) and PAECH et al. (1991) regarded the increase of metamorphism and deformation as an argument for continuity of the section at the northwest corner of Mount Wegener. The assumption of inverse metamorphism without transport (HOFMANN & PAECH 1983) „in the shadow of ... tectonic stress“ is inconsistent with all common concepts of metamorphism. On

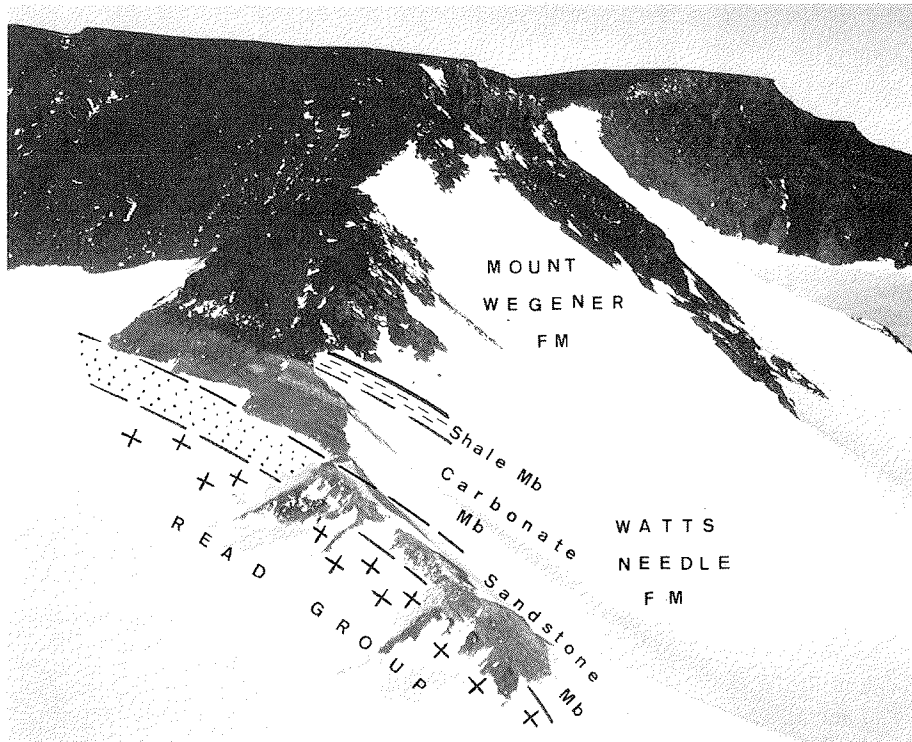


Fig. 5: Mount Wegener, aerial photo; view from the Northwest.

Abb. 5: Mount Wegener, Luftaufnahme mit Blick von Nordwesten.



Fig. 6: Transgression of the Watts Needle Formation over the crystalline basement (Read Group) at Nicol Crags.

Abb. 6: Lagerung der Watts-Needle-Formation diskordant auf dem kristallinen Grundgebirge (Read-Gruppe), Nicol Crags.

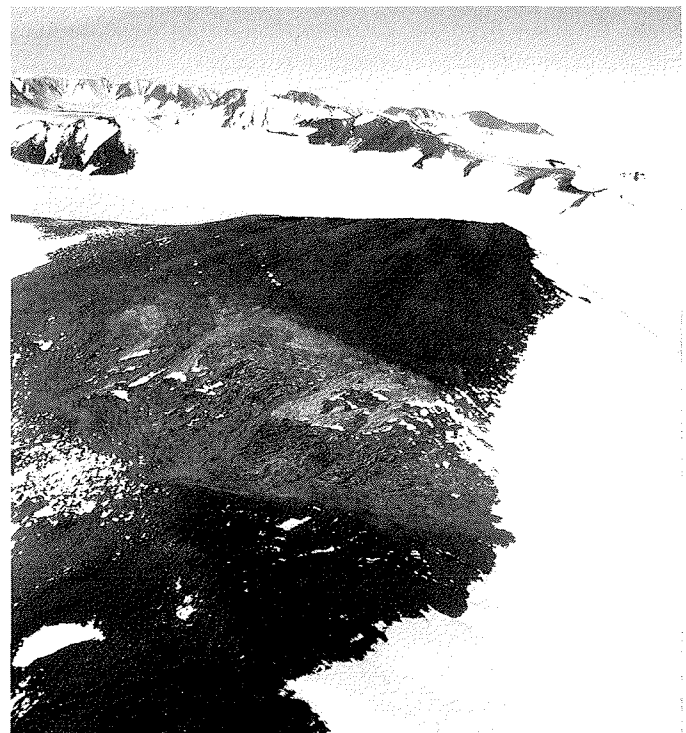


Fig. 7: The Watts Needle from helicopter (view to the East). The lower part consists of crystalline rocks of the Read Group overlain by sandstones and pale colored limestones of the Watts Needle Formation, which is overlain by a large sliver of dark, crystalline rocks (= base of the Mount Wegener Nappe). Imbrication of the Watts Needle Formation to the south.

Abb. 7: Watts Needle vom Hubschrauber aus mit Blick nach Osten. Der untere Teil besteht aus Kristallin der Read-Gruppe, überlagert von Sandsteinen und hellen Kalken der Watts-Needle-Formation, die ihrerseits von einem großen Kristallinschürfling (dunkel, Basis der Mount-Wegener-Decke) überlagert werden. Die Watts Needle-Formation ist an südwärts gerichteten Auf- bis Überschiebungen verschuppt.

the contrary, this so-called inversion is conclusive for the allochthonous position of the hanging wall i.e. the Mount Wegener Formation, forming a nappe called Mount Wegener Nappe. The metamorphism within the Watts Needle Formation was induced from above by the transported heat of the Mount Wegener Nappe.



Fig. 8: Crystalline sliver at the base of the Mount Wegener Nappe, northwest corner of Mount Wegener.

Abb. 8: Kristallinschürfling an der Basis der Mount-Wegener-Decke, NW-Ecke vom Mount Wegener.

The 2-6 μm fractions of samples from the base of the Watts Needle Formation give K-Ar dates between 800 and 520 Ma, that means they are also scattered between the Vendian age of sedimentation and the time of Ross metamorphism. Interestingly, the dates from the $< 0.6 \mu\text{m}$ fractions of these samples cluster about 500 Ma, i.e. apparent Ross ages.

4. THE ALLOCHTHONOUS UNIT (MOUNT WEGENER NAPPE)

The crystalline basement of the Read Mountains (Read Group) and the relics of its sedimentary cover (Watts Needle Formation) are surrounded by very low grade to low grade metasediments of the Mount Wegener Formation (including the former Flett Crags Formation, BUGGISCH et al. 1994).

An Early Cambrian age of sedimentation is verified by fossils and supported by Rb/Sr analyses in the southeastern Read Mountains (PANKHURST et al. 1983, BUGGISCH et al. 1994).

The metamorphism in the Mount Wegener Formation is weak at Trueman Terraces and the nunataks south of Goldschmidt and Lapworth Cirque with illite crystallinities of $\Delta^\circ 2\theta > 0.25$ (very low grade) and it increases continuously to low grade toward north (and northwest). The northern frame of the Read Window is characterized by strong recrystallization of quartz, while feldspar is still brittlely deformed (Fig. 9), and by the formation of newly grown biotite.

The existence of the Mount Wegener Nappe can be evidenced at the northern and southern frame of the Read Window and at the klippen within the Read Window.

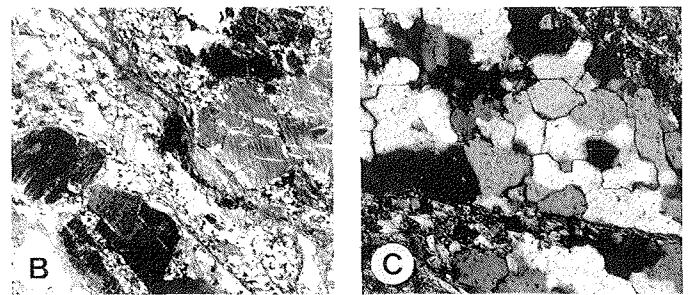
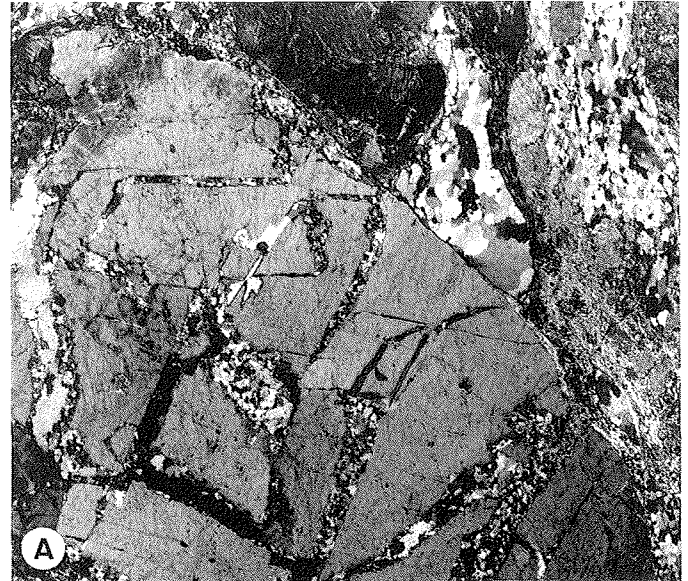


Fig. 9: Augengneis-mylonite from the northern frame of the Read Window. Thin sections showing brittlely deformed feldspar surrounded by dynamically recrystallized quartz. Recrystallization outlasted deformation (straight boundaries and triple junctions of quartz crystals). Sample 88-96; Pol. +, A = x 10; B = x 5; C = x 50.

Abb. 9: Augengneisartiger Mylonit vom Nordrand des Read-Fensters. Dünnschliffe mit spröde deformiertem Feldspat umgeben von dynamisch rekristallisiertem Quarz. Die Rekristallisation überdauert die Deformation; die Korngrenzen der Quarz-Kristalle sind gerade und zeigen Tripelpunkte; Probe 88-96, gekreuzte Nicols, A = x 10; B = x 5; C = x 50.

4.1. The northern frame of the Read Window

The northern frame of the Read Window is exposed at Krebs Nunatak (Figs. 2 and 11). The uppermost parautochthonous granitic rocks of the Read Group are clearly sheared forming „augengneisses“. The hanging allochthonous Mount Wegener Formation (formerly Flett Crags Formation) consists of phyllitic biotite schists and meta-arenites. First tight folds, quartz veins and the first penetrative schistosity are tightly refolded during the second deformation.

Most of the biotite is oriented parallel to s_1 and refolded together with it (Fig. 10A). Nevertheless, undeformed large biotites prove that the growth of new biotite outlasted the first deformation (Fig. 10C). Small biotites can be observed even within s_2 (Fig. 10G). Therefore, it seems most probable that low grade metamorphic conditions persisted until the second deformation.

Step No	Temp. (°C)	$^{40}\text{K}/^{40}\text{Ar}$ (10^{-2})	$^{36}\text{Ar}/^{40}\text{Ar}$ (10^{-6})	$^{37}\text{Ar}/^{39}\text{Ar}$ (10^{-1})	$\text{Ar}_{\text{rad}}/(\text{Ar}_{\text{tot}})$ (%)	$^{39}\text{Ar}/(\Sigma^{39}\text{Ar})$ (%)	Aparent K/Ar date (Ma)
1	500	2869 (20)	106 (44)	0 (4)	96.9 (4)	5.43	500 ± 4
2	550	2586 (20)	47 (14)	2 (4)	98.6 (4)	5.57	560 ± 4
3	600	1454 (9)	3 (5)	2 (2)	99.91 (16)	10.11	909 ± 4
4	620	1257 (10)	15 (4)	2 (2)	99.55 (11)	14.54	1015 ± 6
5	680	1158 (7)	4 (7)	1 (2)	99.88 (21)	15.98	1083 ± 6
6	710	1096 (7)	-1 (4)	2 (2)	100.02 (13)	15.94	1130 ± 5
7	740	1034 (7)	2 (2)	2 (2)	99.93 (6)	14.38	1179 ± 6
8	760	994 (8)	-3 (8)	2 (4)	100.08 (23)	6.22	1215 ± 7
9	780	960 (16)	18 (8)	2 (9)	99.46 (24)	2.63	1240 ± 15
10	800	895 (19)	-8 (22)	0 (14)	100.2 (6)	1.63	1311 ± 21
11	825	891 (9)	52 (16)	7 (13)	98.5 (5)	1.66	1299 ± 11
12	860	885 (19)	33 (179)	4 (14)	99.0 (5)	1.79	1310 ± 21
13	900	900 (11)	-11 (16)	2 (13)	100.3 (5)	1.98	1307 ± 12
14	1100	940 (15)	12 (28)	13 (28)	99.6 (8)	1.64	1261 ± 16
15	1550	3580 (190)	35 (185)	40 (180)	99 (5)	0.48	422 ± 27
total		1196 (3)	9 (2)	9.1 (21)	99.73 (6)	100	1056 ± 2

intralaboratory error ± 3

Tab. 3: Ar-Ar data of siltstone sample 88-242, 2-6 μm from Clayton Ramparts. Argon corrected for mean blank analyses. IUGS-recommended constants (STEIGER & JÄGER 1977) are used. If not otherwise stated, the quoted errors are intra-run analytical uncertainties at a level of 95 % confidence. Those in parentheses refer to the last digit(s).

Tab. 3: Ar-Ar-Daten der Siltsteinprobe 88-242, 2-6 μm von Clayton Ramparts.

The decollement between the Read Group and the Mount Wegener Nappe is marked by a mylonite zone (Fig. 11) containing cm- to m-thick shear bodies of mylonitized pelites, sandstones, conglomerates and crystalline basement rocks. Quartz clasts and crystals are ductilely deformed and strongly recrystallized, new biotite has grown, while cracks of brittlely broken feldspars are healed with quartz (Fig. 9). The dynamic recrystallization of quartz during mylonitic deformation was outlasted by almost static recrystallization as shown by the weak undulatory extinction of new quartz and straight grain boundaries in stress-sheltered areas (Fig. 10B).

Ideal conditions for K/Ar analysis exist only if exclusively new mica is measured which was formed during a defined process and if no later alteration or overprint occurred. This is more or less true for the 2-6 μm fractions of low-grade metamorphic biotite schists and phyllites of the northern frame of the Read Window (Fig. 10A-E) and for samples of the Wyeth Heights Formation cropping out close to the northern thrust boundary. These rocks give rather consistent dates of about 490 Ma (505 to 483 Ma, Fig. 2). A similar date of 492 Ma (Fig. 1) is determined for the same fraction of a mica schist of the Stratton Group from Williams Ridge (Williams Ridge Formation according to MARSH 1983b).

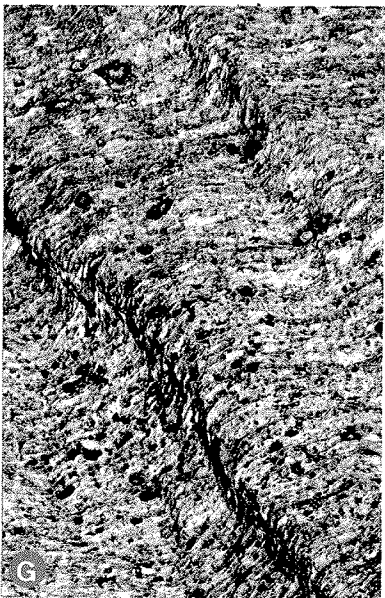
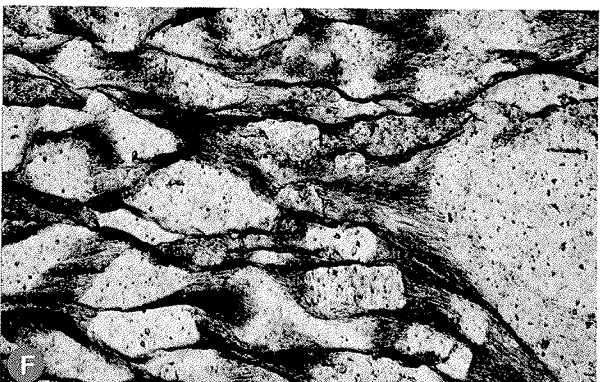
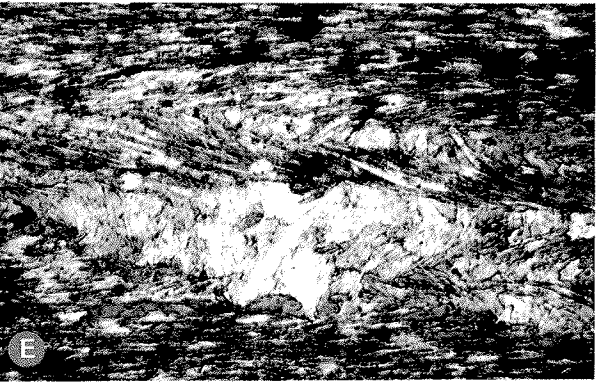
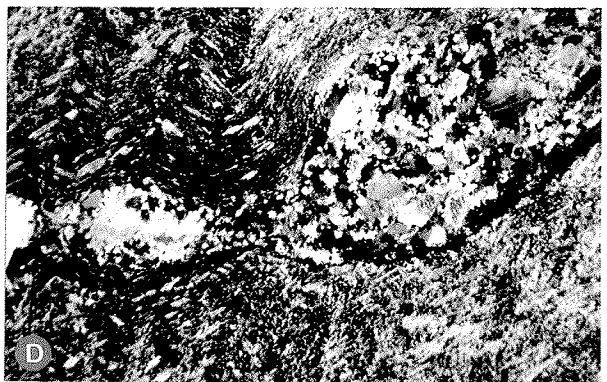
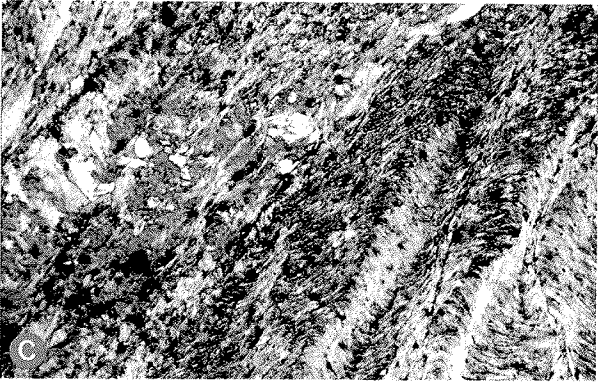
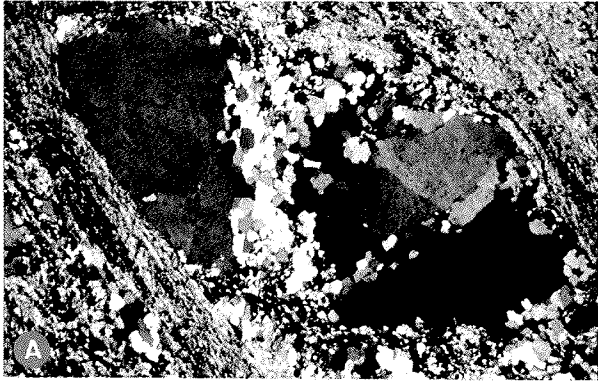
This age probably documents the metamorphic overprint of the Stratton and Pioneer Groups and the transport of the Mount Wegener Nappe, both of which are related to D_2 and to the late Ross Orogeny. The younging of the fine grained fractions can be artificial. But interestingly the date of about 245 Ma of the < 0.2 μm fraction from the northern frame of the Read window (Fig. 4) is in the rank of apatite fission track dates.

4.2. The southern frame of the Read Window

The southern frame of the Read Window is exposed at the northern and northwestern slope of Mount Wegener (Fig. 12). Almost undeformed granitic rocks of the Read Group are unconformably overlain by the Watts Needle Formation. Within the upper part of the Limestone Member of this formation a weak cleavage is developed which becomes more pronounced upwards in the overlying Shale Member. This cleavage, which correlates to the emplacement of the Mount Wegener Nappe corresponds to the second cleavage (s_2) in the Mount Wegener Formation.

The main decollement of the Mount Wegener Formation is marked by a shear zone with metre-sized slabs of granitic basement rocks (Fig. 8). Whether these crystalline rocks are abraded fragments of the Read Group or represent an unknown basement of the Mount Wegener Formation is still under discussion.

Above the decollement zone, the Mount Wegener Nappe is multiply deformed (Fig. 13). The pelites, lithic arenites and polymict conglomerates of the Mount Wegener Formation are tightly folded (development of B_1). Limestone clasts are extremely stretched while feldspars are brittlely deformed. Quartz clasts and folded quartz veins exhibit grain boundary migration and formation of subgrains. The growth of new phyllosilicates - predominantly illite/sericite and chlorite but also a minor amount of biotite - in beards (within arenites) and in shear planes (within pelites) - led to the formation of a penetrative schistosity (s_1) during the first deformation. The amount of biotite appears to increase towards the plateau of Mount Wegener



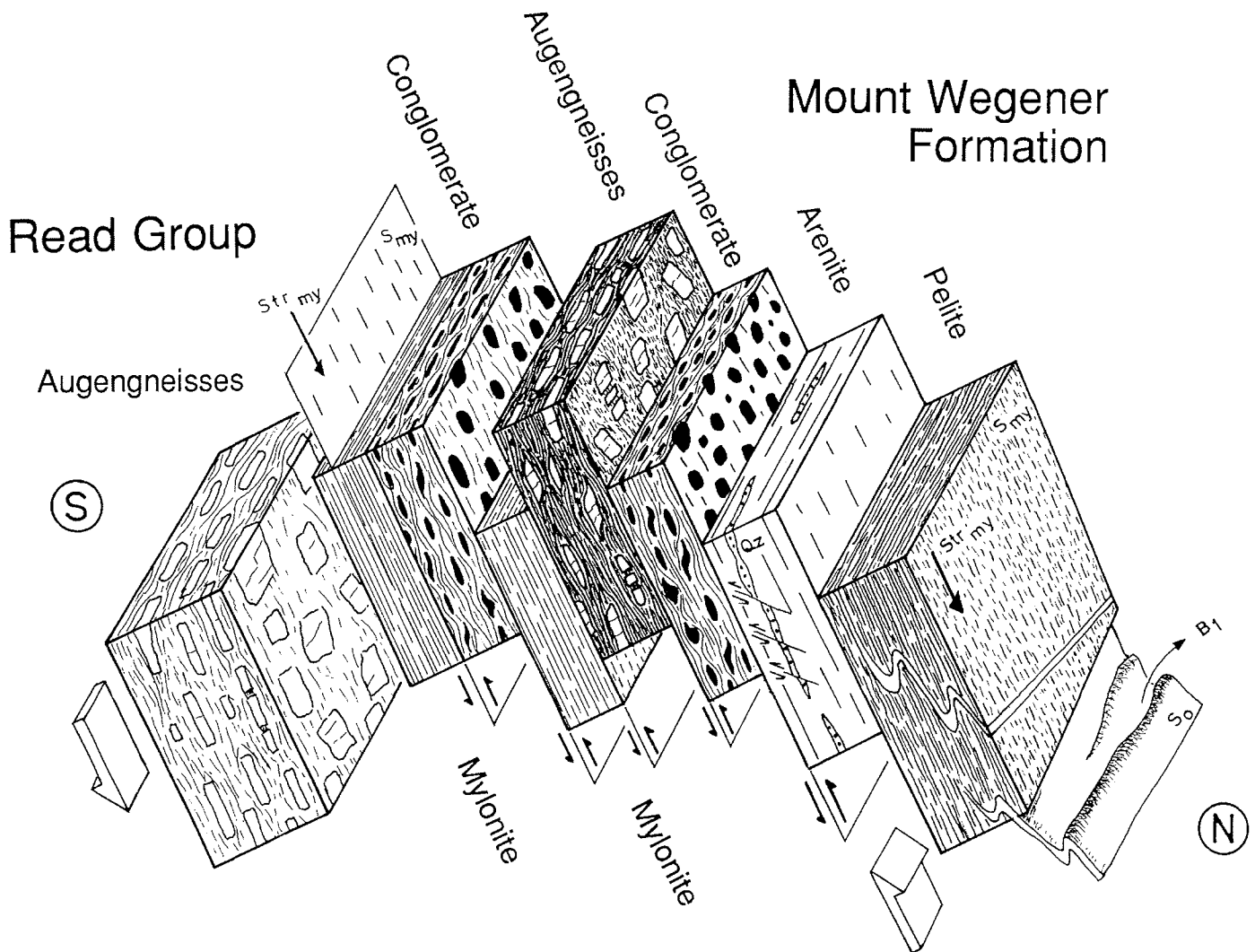


Fig. 11: Structure of the northern frame of the Read Window at Krebs Nunatak.

Abb. 11: Mylonitische Gefüge an der Nordgrenze des Read-Fensters am Krebs-Nunatak. S_{my} = mylonitisches „S“, Str_{my} = mylonitische Streckungsfaser.

Fig. 10: Thin sections of metasediments from the Mount Wegener and the Wyeth Heights Formations.

A = Mylonitic conglomerate, Mount Wegener Formation, from the northern frame of the Read Window. Quartz clasts are stretched and recrystallized. Krebs Nunatak, sample 88-96; Pol. +; width of fig. = 3.5 mm. B = Metasandstone, Mount Wegener Formation, from the northern frame of the Read Window. Quartz is dynamically recrystallized. Static annealing outlasted deformation and produced 120° triple points in quartz boundaries. Growth of biotite/chlorite/quartz pressure-shadow beards. Sample 88-44; Pol. +; width of fig. = 0.8 mm. C = Metapelite, Mount Wegener Formation, from the northern frame of the Read Window. s_1 - marked by biotite and chlorite - was refolded during D_2 . s_2 -planes steeply dipping towards left. Growth of biotite outlasted D_1 , Niggli Nunatak, sample 88-36; Pol. +; width of fig. = 3.5 mm. D = Metapelite, Mount Wegener Formation, from the northern frame of the Read Window. s_1 quartz veins are deformed by boudinage and completely recrystallized. s_1 - marked by biotite and chlorite - was refolded during D_2 . Sample 88-47; Pol. +; width of fig. = 3.5 mm. E = Metapelite, Mount Wegener Formation, from the northern frame of the Read Window. s_2 (s_1 ?) was isoclinally refolded. Growth of phyllosilicates outlasted deformation. Sample 88-47b; Pol. +; width of fig. = 0.8 mm. F = Metaarenite, Wyeth Heights Formation. Quartz grains are flattened by pressure solution. Growth of serizite/chlorite/quartz beards. Sample 88-179; plane light; width of fig. = 0.8 mm. G, H and I = Metapelite/arenite from Wyeth Heights Formation. s_0 is marked by layers of quartz sand; penetrative s_1 cuts older s_x (Fig. G and H) and is, in turn, cut by s_2 . Incipient growth of biotite in s_2 (Fig. G). Sample 88-168; Fig. G = plane light; length = 0.8 mm; Fig. H and I = Pol. x and plane light; width = 3.5 mm.

Abb. 10: Dünnschliffe von Metasedimenten der Mount-Wegener-Formation und Wyeth-Heights-Formation.

A = Mylonitisches Konglomerat, Mount-Wegener-Formation, vom Nordrand des Read-Fensters. Gestreckte und rekristallisierte Quarzklasten. Krebs-Nunatak; Probe 88-96, gekreuzte Nicols, Bildbreite = 3,5 mm. B = Metasandstein, Mount-Wegener-Formation, vom Nordrand des Read-Fensters. Dynamisch rekristallisierter Quarz, statische Ausheilung überdauerte die Deformation und führte zu 120° -Tripel-Punkten der Quarzkornengrenzen. Druckschattenhöfe aus Biotit/Chlorit/Quarz. Probe 88-44, gekreuzte Nicols, Bildbreite = 0,8 mm. C = Metapelit, Mount-Wegener-Formation, vom Nordrand des Read-Fensters. s_1 markiert durch Biotit und Chlorit wird durch D_2 wiedergefaltet. s_2 fällt steil nach rechts. Biotitwachstum überdauert D_1 . Niggli Nunatak; Probe 88-36, gekreuzte Nicols, Bildbreite = 3,5 mm. D = Metapelit, Mount-Wegener-Formation, vom Nordrand des Read-Fensters. s_x (s_1 ?) ist isoklinal wiedergefaltet. Phyllosilikatwachstum überdauert die Deformation. Probe 88-47b, gekreuzte Nicols, Bildbreite = 0,8 mm. F = Meta-Arenit, Wyeth-Heights-Formation. Quarzkörner durch Drucklösung geplättet. Bildung von Serizit-/Chlorit-/Quarzfaserbärten in Druckschattenhöfen. Probe 88-179, einfach pol. Licht, Bildbreite = 0,8 mm. G, H und I = Metapelit-/Arenit, Wyeth-Heights-Formation. s_0 markiert durch Quarzsandlagen. Penetratives s_1 durchschneidet älteres s_x und wird seinerseits von s_2 durchschnitten. Beginnendes Biotitwachstum in s_2 . (G) Probe 88-168, einfach pol. Licht, Bildbreite 0,8 mm. (H und I) Probe 88-168, gekreuzte Nicols und einfach pol. Licht, Bildbreite 3,5 mm.

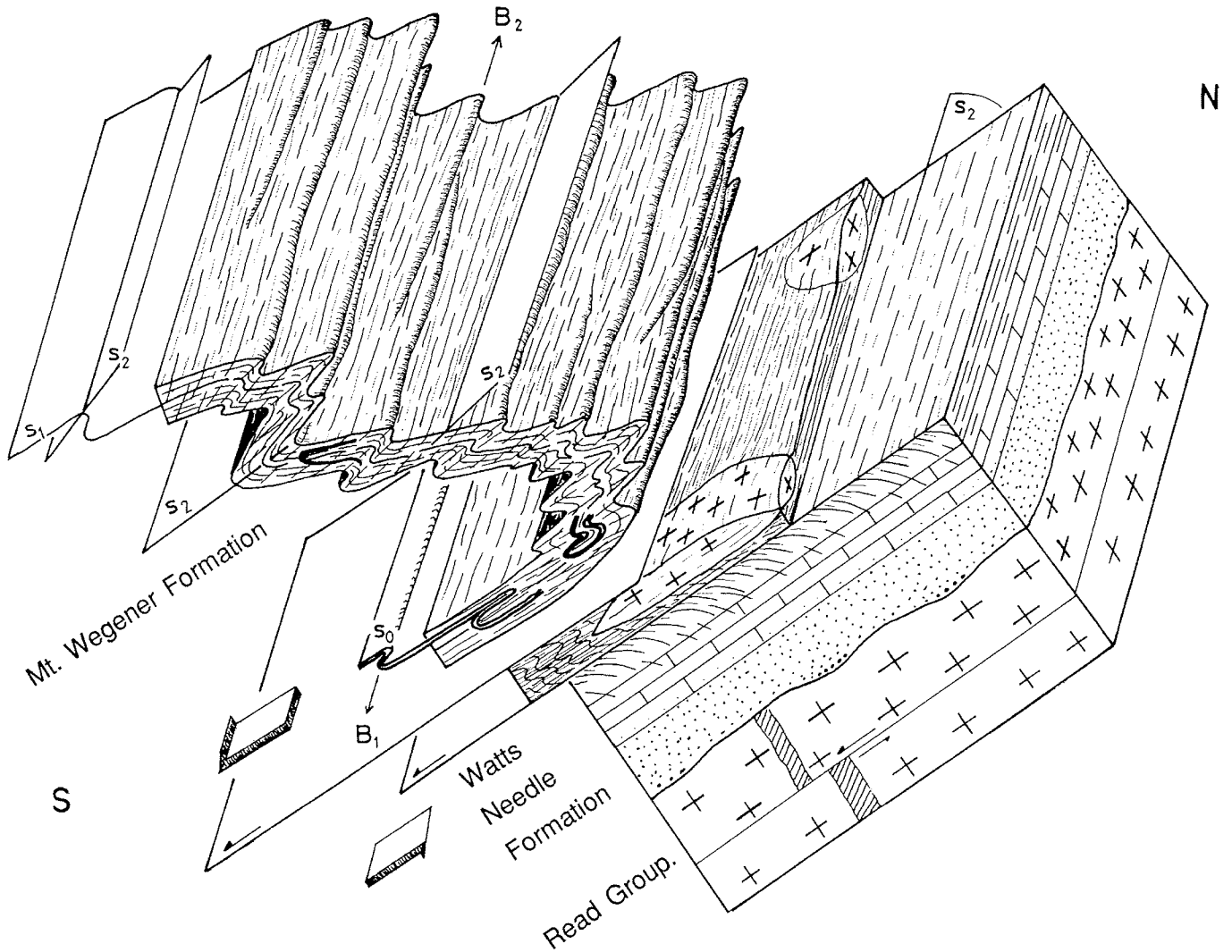


Fig. 12: Structure of the southern frame of the Read Window at the northwest corner of Mount Wegener.

Abb. 12: Überschiebungsgefüge an der Südgrenze des Read-Fensters an der NW-Ecke des Mount Wegener.

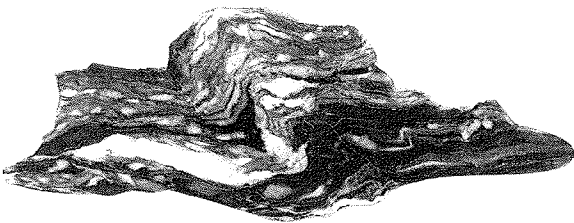


Fig. 13: Conglomerate of the Mount Wegener Formation. Carbonate clasts are extremely stretched in s_1 during the isoclinal folding (D_1). s_1 was refolded by D_2 . Polished slab; Lapworth Cirque; sample 88-104, x 0.65.

Abb. 13: Konglomerat der Mount-Wegener-Formation. Karbonatklasten sind während der isoklinalen Faltung D_1 extrem in s_1 gestreckt. s_1 ist durch D_2 wiedergefaltet. Poliertes Handstück von Lapworth Cirque, Probe 88-104, x 0,65

pointing to imbrication within the Mount Wegener Nappe. The schists were refolded to recumbent open folds facing towards the south during the second deformation. A distinct second

crenulation cleavage (s_2) can be observed. The second folds probably developed during the final emplacement of the Mount Wegener Nappe.

In contrast to CLARKSON'S (1983) conclusions, all shear sense criteria, i.e. the geometry of minor folds, phacoids of allochthonous basement slivers, phacoidal imbrication or quartz veins, sigma and delta clasts, and shear bands prove southward directed transport. The plot of the structural data of the Mount Wegener Thrust (Fig. 14) shows, that thrusting generally is orthogonal, and that - on average - sense of shear is roughly top-to-south directed. This is slightly focussed by ironing out the Read Window anticline (Fig. 15). But this process does not produce a meaningful result: The main Mount Wegener Thrust seems to be an intensified s_2 , as thrusting is mainly using the s_2 planes of the Mount Wegener Formation (Fig. 16), apart from those s_2 planes which are out of function. And these secondary thrusts above the master thrust are generally north-dipping at the southern limb of the Read Window anticline. After unfolding and rotation, these north-dipping thrusts would show a southerly dip and a northward overthrusting sense of movement (Fig. 15).

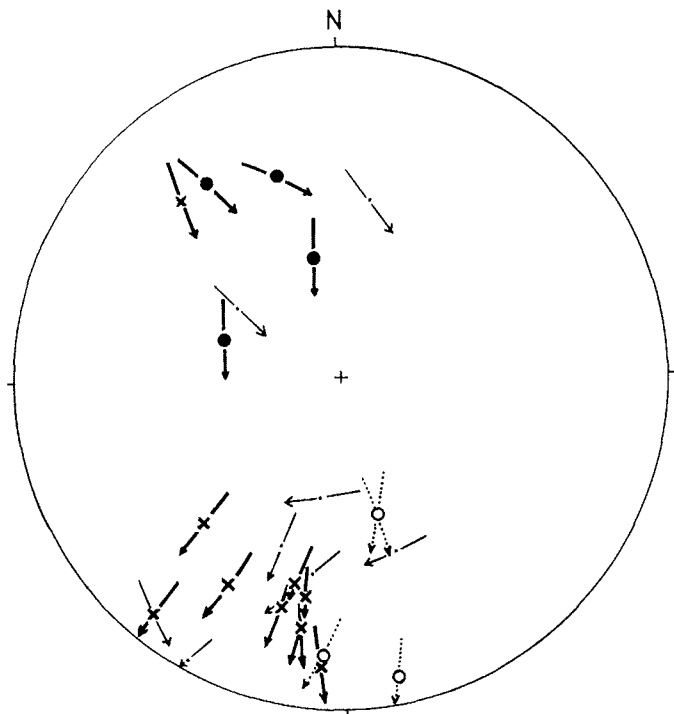


Fig. 14: So called Hoeffner diagram (uncorrected), Read Window /Mount Wegener Thrust: poles to thrust planes, transport directions, and sense of shear (arrows). Northern limb of the Read Window anticline: poles = crosses with thick arrows; southern limb of Read Window anticline: poles = solid dots with thick arrows (poles = small dots with thin arrows: upward thrusting at southern limb); central part of window (foot of Gora Rudachenka): duplex system: poles = circles with dotted arrows. Reconstruction of Hoeffner diagram according to HOEPPNER (1955).

Abb. 14: Sogenanntes Hoeffner-Diagramm (nicht korrigiert), Read-Fenster, Mount-Wegener-Überschiebung. Pole der Überschiebungsflächen, Transportrichtung und Schersinn (Pfeile); Nordschenkel der Read-Fenster-Antiklinale, Pole = Kreuze mit fettem Pfeil; Südschenkel der Read-Fenster-Antiklinale, Pole = große Punkte mit fettem Pfeil; (Pole aufwärts gerichteter Überschiebungen am Südschenkel = kleine Punkte mit dünnem Pfeil), Zentrum des Fensters (am Fuße der Gora Rudachenka), Duplex-Zone, Pole = Kreise mit gepunktetem Pfeil. Konstruktion von Hoeffner-Diagrammen nach HOEPPNER (1955).

Altogether, that means that thrusting and formation of the Read Window anticline is more or less coeval. And thrusting outlasted formation of the anticline at least in the south as indicated by the north-dipping s_2 -planes showing southward transport.

K-Ar dates for the rocks forming the southern frame of the Read Window, e.g. from the northwestern slope of Mount Wegener, are somewhat older than for rocks on the northern frame. This is probably related to the lower grade of metamorphism (partly recrystallization of quartz, but almost no formation of biotite) and was interpreted by BUGGISCH et al. (1990) as white mica age of the first penetrative deformation. Younging of the dates is observed toward the finer grain fractions.

Samples of the Mount Wegener Formation (Fig. 2) from the southern slope of Mount Wegener and east of it (Truman Terraces, Swinnerton Ledge) give dates increasing eastwards from 510 to 550 Ma which apparently represent mixtures of inherited Lower Cambrian ages of sedimentation/diagenesis and the very low-grade metamorphism of the Ross Orogeny. The dates

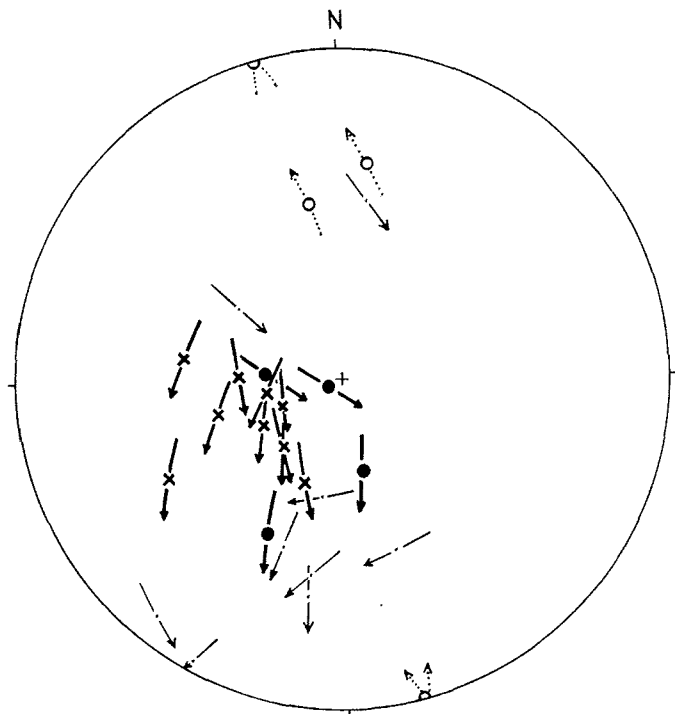


Fig. 15: Hoeffner diagram, similar to Fig. 14, but corrected (northern limb of Read Window anticline rotated 50° towards the South, i.e. minimum dip of s-planes on the northern limb; southern limb rotated 55° towards N, i.e. dip of unmetamorphosed Watts Needle Formation; central part of window is not rotated). Symbols as in Fig. 14. See text for further explanation.

Abb. 15: Hoeffner-Diagramm (ähnlich Abb. 14) korrigiert (Nordschenkel der Read-Fenster-Antiklinale um 50°, d.h. das Mindesteinfallen der s-Flächen am Nordschenkel, nach S rotiert; Südschenkel um 55°, d.h. das Einfallen der nicht metamorphen Watts-Needle-Formation, nach N rotiert; Zentrum des Fensters nicht rotiert). Symbole wie in Abb. 14; weitere Erläuterungen im Text.

of the $< 0.6 \mu\text{m}$ fractions are in the range of the age of metamorphism in the northern Read Mountains (Fig. 4).

4.3. Klippen within the Read Window

The Watts Needle (and Werner Nunatak) is situated in the inner part of the Read Window (Fig. 2). Here, the crystalline basement of the Read Group is unconformably overlain by sandstones and limestones of the Watts Needle Formation (Fig. 7). Whereas the Sandstone Member is nearly undeformed, deformation increases within the Limestone Member towards the overlying almost horizontal thrust sheet forming south to southwestward directed vergent folds and imbrications. The summit of the Watts Needle consists of about 100 m thick cataclastic orthogneisses with mafic dykes. These crystalline basement rocks correspond to the granitic slabs at the base of the Mount Wegener Nappe on Mount Wegener itself. Hence, the orthogneisses on top of Watts Needle form a typical „klippe“ of the Mount Wegener Nappe within the Read Window. The provenance of the crystalline basement (abraded Read Group or unknown basement from beneath the Mount Wegener Formation) is not clear.

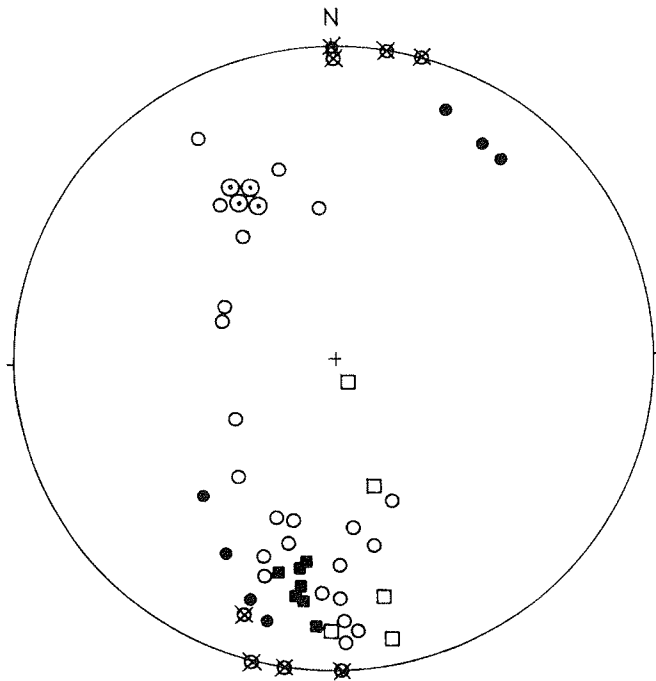


Fig. 16: Schmidt net: poles to s-planes used by thrusting: solid symbols : northern limb of the Read Window anticline; open symbols: southern limb of the Read Window anticline; squares = s_1 ; dots, circles = s_2 ; crossed = out of function; Circles with dot = s_1 in unmetamorphosed sediments of Watts Needle Formation. See text for further explanation.

Abb. 16: Schmidtsches Netz. Pole von s-Flächen, die von der Überschiebungstektonik benutzt wurden; kompakte Symbole = Nordschenkel der Read-Fenster-Antiklinale; offene Symbole = Südschenkel der Read-Fenster-Antiklinale; Quadrat = s_1 ; Kreis u. Punkt = s_2 , durchkreuzt = außer Funktion geraten; Kreis mit Punkt = s_1 in den unmetamorphosen Sedimenten der Watts-Needle-Formation; weitere Erläuterungen im Text.

4.4. The structure of Stephenson Bastion

The northern boundary of the Mount Wegener Nappe and the medium to high grade metamorphic rocks of the Northern Belt of the Shackleton Range (see BUGGISCH et al. 1994) is in turn a southerly directed thrust system, called the Otter Highlands Thrust. It is exposed around Y-Nunatak (Fig. 27) in the southern Otter Highlands and appears to be present at the northern margin of Stephenson Bastion (Clayton Ramparts).

The Stephenson Bastion Formation in general forms a large E-W-trending open syncline (CLARKSON 1983). But in detail, there are many special folds and related structures indicating southward directed tectonic transport on Stephenson Bastion.

At the eastern end of Clayton Ramparts, quartz clasts in conglomerates exhibit strong dynamic recrystallization at grain boundaries while feldspars show brittle deformation. Triple junctions with angles of 120° are evidence that quartz recrystallization outlasted the deformation. The dominant phyllosilicate in beards is chlorite, but incipient growth of biotite also occurs. To the south deformation and (low- to very low-grade) metamorphism decrease. Sandstones at Ram Bow Bluff are only affected by strong pressure solution of quartz and formation of chlorite/(illite)/ quartz beards (Fig. 10F).

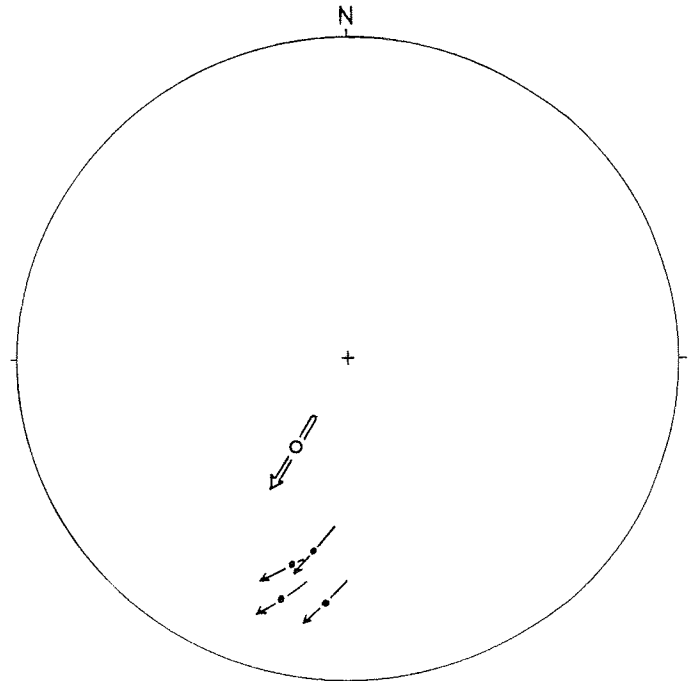


Fig. 17: SW-ward directed tectonic transport at Clayton Ramparts/northern Stephenson Bastion: measurement of thrust-parallel inverted s-planes (dots), related stretching lineations (direction of arrows) and sense of thrusting movements (heads of arrows) (Hoeppener diagram); open symbols = thrust 2 km south of Clayton Ramparts.

Abb. 17: Südwestwärtiger tektonischer Transport by Clayton Ramparts und in der nördlichen Stephenson Bastion. Meßwerte von überkippten, überschiebungsp parallelen s-Flächen (Punkte), zugehörige Streckungslineare (Lage der Pfeile) und Bewegungssinn der Überschiebung (Pfeilspitze); Hoeppener-Diagramm, Abb. 14; offene Symbole = Überschiebung 2 km südlich Clayton Ramparts.

At Clayton Ramparts, the northern limb of the Stephenson Bastion syncline clearly shows that the pelites, crossbedded quartzites and conglomerates are overturned ($s_0 = 010/50$ to $010/75$). The stretching lineation is roughly N-S (Fig. 17); both overturning and stretching point to the proximity of the Otter Trust.

The Stephenson Bastion syncline seems to be a rather simple one in the northern part of the Ram Bow Bluff area (Fig. 18). The northernmost part shows moderately south-dipping bedding ($s_0 = 200/4$), becoming more gentle some 500 m to the south ($s_0 = 185/25$, $195/15$), then horizontal, passing into a northward dip further to the south ($s_0 = 020/15$, $040/30$). Still further south, tighter folds have amplitudes and wave length of some 20-50 m. These folds show a weak vergence to the south (axial plane = 020 to $040/85$). This vergence is consistent with the behaviour of the cleavage: (i) In places, cleavage is developed in two conjugated sets in coarser rock types (quartzites). Both sets are north-dipping $s_{1s} = 030/70$; $s_{1a} = 030/80$, (terminology according to VOLL 1960). (ii) Cleavage refraction is sometimes unusual at first sight. Instead of becoming closer to the axial plane in the finer grained (pelitic) than in the coarser grained (quartzitic) rock types, cleavage in the pelites in the southern limb shows a strong refraction towards the south, i.e. an increase of the angle between axial plane and cleavage! This indicates considerable rotation of the cleavage system towards south which is consistent

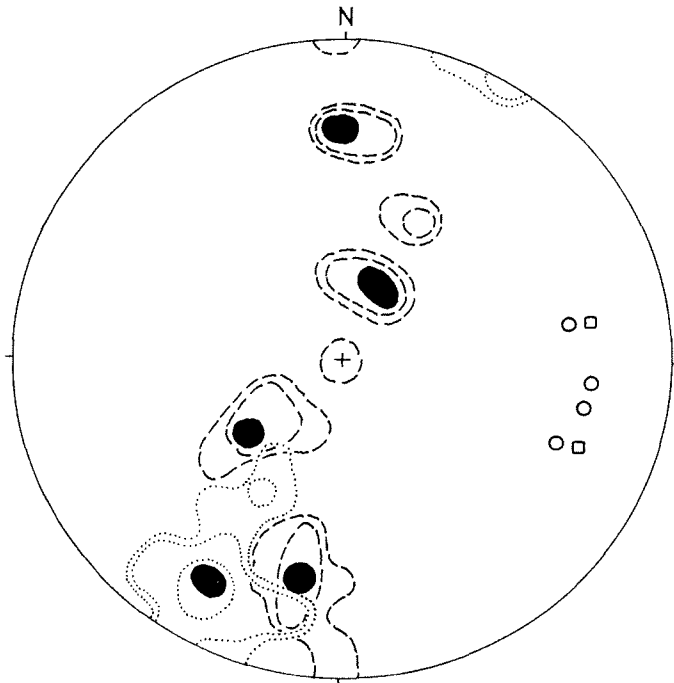


Fig. 18: s_0 , s_1 , B_1 , and B_2 values from Stephenson Bastion, plotted on a Schmidt net; s_0 = dashed contours (3-6-9-12 %, $n = 36$); s_1 = dotted contours (9-18-27-36 %, $N = 30$); B_1 = open circles, B_2 = squares.

Abb. 18: s_0 , s_1 , B_1 - und B_2 -Messwerte aus der Stephenson Bastion im Schmidt-Netz. s_0 = gestrichelte Isolinien (3-6-9-12 %, $n = 36$); s_1 = gepunktete Isolinien (9-18-27-36 %, $n = 30$); B_1 = offene Kreise; B_2 = Quadrate.

with southward tectonic transport as a whole. Southward thrusting is observed repeatedly in the Ram Bow Bluff area, indicated by quartz feather-joints and slickensides. The thrust planes are horizontal or dip gently north (070/13, 030/25, Fig. 19). Offsets in the range of some 20 cm were measured. It is still open to question, whether this thrusting was coeval with folding and cleavage formation or took place later, and therefore it is open to question, whether it is of Ross age or older.

The style of folding was observed to be similar in the western and central parts of Stephenson Bastion south of Clayton Ramparts. It is somewhat unclear because a second phase of deformation (D_2 with B_2 and s_2) has overprinted the original D_1 -structures not only in incompetent rock types, but also in quartzitic ones. Because the close trend of both, the B_1 - and B_2 -axes are subparallel, the general structure of Stephenson Bastion appears rather simple (Fig. 18). The vergence and a shear zone (030/25) indicate again a southward tectonic transport (Fig. 17). Main Structures of Stephenson Bastion are summarized in Figures 18 and 20.

Plots of „IC“ versus grain size (Fig. 3) indicate that the mica/clay associations of samples from Stephenson Bastion (and Wyeth Heights) differ from those of the Mount Wegener Formation. K-Ar dates of the 2-6 μm fractions are between 1050 and 940 Ma (Fig. 4). These pre-Ross dates are probably related to the formation of chlorite/illite/quartz beards in siltstones at Ram Bow Bluff and Clayton Ramparts. No younging is observed in the 0.6-2 μm fractions of Ram Bow Bluff, whereas the

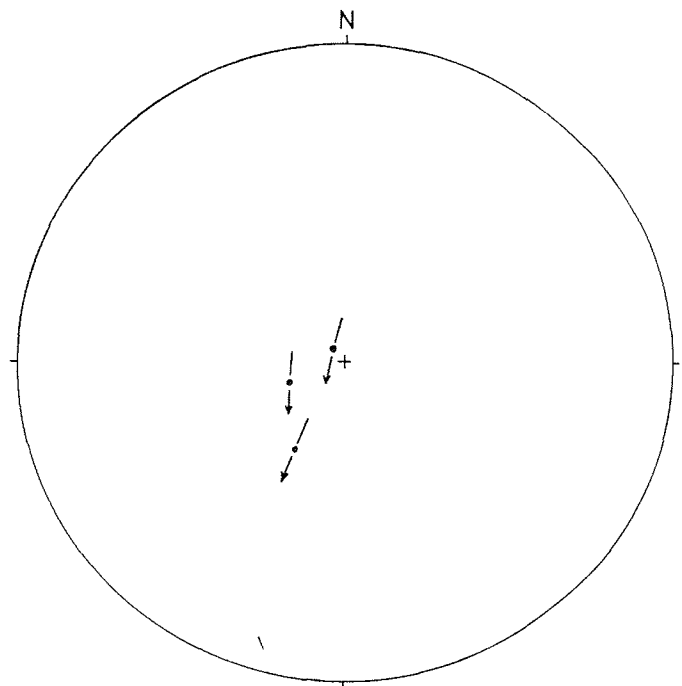


Fig. 19: Minor southward directed thrusts of Ram Bow Bluff area in the Hoeppener diagram (compare Fig. 14 and 17); dots = thrust planes; arrows = thrust directions (slickensides, stretching lineations); heads of arrows = sense of shear.

Abb. 19: Kleine, südwärts gerichtete Überschiebungen im Rambow-Bluff-Bereich im Hoeppener-Diagramm (vgl. Abb. 14 und 17); Punkt = Überschiebungsfläche; Pfeil = Überschiebungsrichtung (Harnisch-, Streckungslineation); Pfeilspitze = Überschiebungssinn.

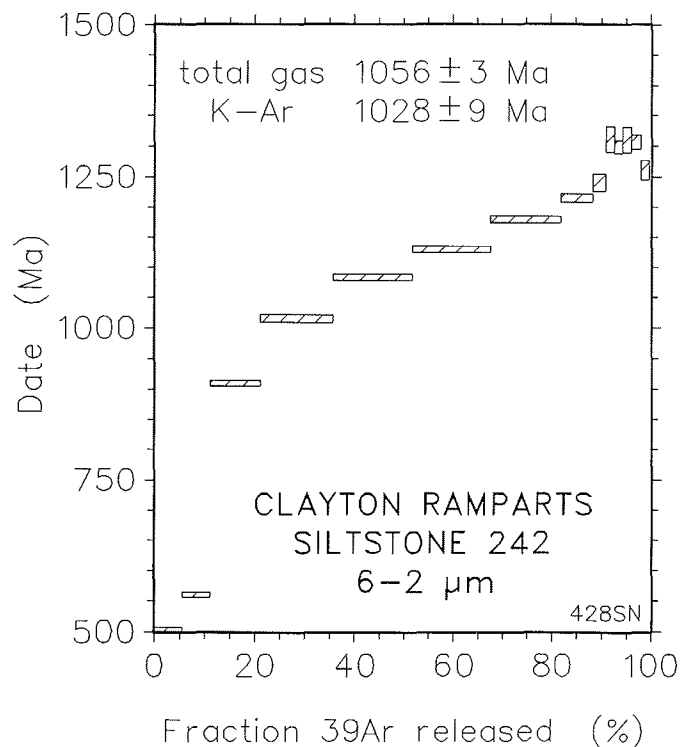


Fig. 20: $^{38}\text{Ar}/^{40}\text{Ar}$ age spectrum of the 2-6 μm fraction of siltstone sample 88-242; Clayton Ramparts.

Abb. 20: $^{38}\text{Ar}/^{40}\text{Ar}$ -Altersspektrum der 2-6 μm -Fraktion der Siltsteinprobe 88-242 von Clayton Rampart.

equivalents from Clayton Ramparts are about 100 Ma younger than the 2-6 μm fractions. Like the < 2 μm fractions of the samples from the late Proterozoic Wattle Needle Formation, K-Ar dates of the < 0.2 μm fractions from Clayton Ramparts are only little younger than the Ross Orogeny.

$^{40}\text{Ar}/^{39}\text{Ar}$ incremental degassing techniques were applied to a single sample (242) from Clayton Ramparts (Tab. 3, Fig. 20), although fine-grained samples are not very suitable owing to probable recoil losses and interferences caused by nuclear reactions during neutron irradiation. In fact, the difference between the conventional date of 1028 Ma and the Ar-Ar total gas date of 1056 Ma indicates losses of Ar^{39} of about 3.5 %. The drop in the apparent ages of the highest-grade increments indicates interferences. Despite these uncertainties the monotonously increasing apparent ages suggest partial argon loss due to volume diffusion and/or newly formed, fine-grained minerals. The first two low-temperature increments with 10 % of the total gas release could be explained by very fine-grained illite formed or reset at about 0.5 Ga, and the high-temperature steps indicate a primary age of more than 1230 Ma. The release pattern could well be explained by a single thermal event during Ross times.

We favour the following hypothesis. The 1250 Ma Rb-Sr isochrone (BUGGISCH et al. 1994) of samples from the Stephenson Bastion Formation is interpreted as age of diagenesis or sedimentation which is corroborated by acritarchs from Mount Greenfield (WEBER 1991). These Late Precambrian sediments suffered low-grade to very low-grade Precambrian metamorphism which led to the formation of illite/chlorite/quartz beards and the growth of new phyllosilicates. This metamorphism is regarded as the main reason for the scattered K-Ar dates of about 1000 Ma and the onset of the gentle 900-1250 Ma slope in the Ar-Ar age spectrum of sample 242. Close to the northern boundary of the Mount Wegener Nappe at the overturned limb at Clayton Ramparts the Precambrian metamorphism is overprinted by the Ross Orogeny leading to a strong younging of the K-Ar dates of the fractions 0.6-2 μm and in part of the initial steps of the age spectrum of the 2-6 μm fraction of sample 242. The effect of this overprint decreases toward the south so that no younging of K-Ar dates is observed in the 0.6-2 μm fraction of samples from Ram Bow Bluff.

4.5. Crystalline mass of unknown provenance

A mass of crystalline rocks of unknown provenance is exposed west of Stephenson Bastion (BUGGISCH et al. 1994, Fig. 4). The medium or high grade metamorphic meta-gabbros do not fit - up to now - any model. North of it, southward dipping metaclastics are exposed in two isolated nunataks south of the Fuchs Dome. Meta-conglomerates containing abundant relict grains of quartz and feldspar (predominantly microcline) and sandstones show mylonitic structures. More than 50 % of the quartz is dynamically recrystallized, weak undulatory extinction of new quartz grains and preserved straight grain boundaries prove the persistence of high temperatures up to the end of deformation.

Phyllosilicates consist mainly of white mica, but incipient growth of biotite is also observed.

4.6. The northern boundary of the Mount Wegener Nappe

The northern boundary of the Mount Wegener Nappe adjacent to the crystalline rocks of the northern belt of the Shackleton Range (Pioneer and Stratton Groups) is exposed at Y-Nunatak in the southern Otter Highlands, where medium to high grade metamorphic rocks are thrust southward and orthogonally over the low-grade metamorphic Wyeth Heights Formation (Otter Highlands Thrust, KLEINSCHMIDT et al. 1992), (Figs. 21 and 27).

This boundary was regarded as normal fault by CLARKSON (1972, 1982). But already MARSH (1983a) assumed southward thrusting on the basis of the sequences and strike and dip. Evidence for southward thrusting, i.e. thrusting of the northern belt over the Wyeth Heights Formation, is given by the following indications from Y-Nunatak and the next spur to the west:

Both units, the low-grade and the basement rocks are mylonitized close to the thrust system. The mylonites of the Wyeth Heights Formation are characterized by southward directed shear bands (Fig. 22). Vergence and attitude of long-short limbs of minor B_2 -folds, transposition and imbrication of quartz veins paralleling s_1 indicate the same kinetics. Moreover, B-axes of minor first folds are more or less rotated into the tectonic

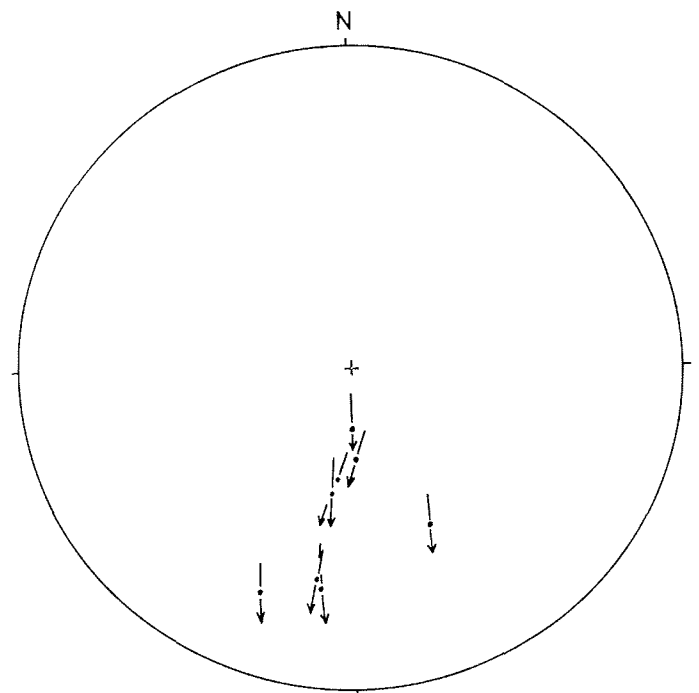


Fig. 21: HOEPPENER diagram (see Fig. 14), Otter Highlands Thrust at Y-Nunatak (southern Otter Highlands), showing poles of thrust planes (dots), transport directions and sense of shear (arrows), indicating southward thrusting nearly orthogonal to the thrust plane.

Abb. 21: HOEPPENER-Diagramm (s. Abb. 14), Otter-Highlands-Überschiebung beim Y-Nunatak (südliche Otter-Highlands); Punkte = Pole der Überschiebungsflächen; Pfeile = Transportrichtung und Schersinn; Überschiebungsrichtung nahezu normal zum Streichen der Überschiebungsfläche.



Fig. 22: Otter Highland Thrust, south of Y-Nunatak; shear bands indicate southward displacement. Left = South; right = North.

Abb. 22: Otter-Highlands-Überschiebung südlich Y-Nunatak; Scherbänder als Beleg für Südtransport des Hangenden (links = Süden, rechts = Norden).

transport direction (Fig. 23). In general, nearly all rocks of the Wyeth Heights Formation (apart from the quartzites at Wyeth Heights itself) have been deformed at least twice. B_2 is horizontal and strikes E-W (Fig. 23), B_2 and s_2 are related to the thrusting, and B_1 was passively affected by this process.

Structures of the mylonites of the basement rocks show consistent behaviour, southward movement is indicated by book shelf structures of sheared feldspars (Fig. 24), asymmetric feldspar augen (sigma-clasts), (Fig. 25), crosscutting pegmatitic veins have been sheared off (Fig. 26), and metre-sized slivers of quartzites and schists of the Wyeth Heights Formation are incorporated into the basal parts of the overlying sheet.

Metamorphism and deformation decrease within phyllites, slates and arenites of the Wyeth Heights Formation from north to south. Close to the northern boundary, quartzites exhibit a strong mylonitic fabric. More than 50 % of quartz is dynamically recrystallized. In metapelites most of the phyllosilicates, e.g. white mica, biotite and minor amounts of chlorite, are parallel to the penetrative cleavage of D_1 . Schistosity s_1 is usually parallel or subparallel to s_0 , which seems to be isoclinally folded before (?) or during D_1 . A weak crenulation cleavage (s_2) developed during D_2 which refolded s_1 (Fig. 10G-H). In few samples an older schistosity (s_x) is still preserved (Fig. 10I).

Biotite disappears toward the south. In the quartzites of Wyeth Heights, quartz grains are flattened by strong pressure solution and formation of quartz/sericite/chlorite beards. Incipient recrystallization of quartz can be observed.

The biotite phyllites close to the northern boundary of the Mount Wegener Nappe yielded K/Ar dates which are in accordance with the Ross Orogeny. The date of 548 Ma from sample 173 (Tab. 2) seems to be partly inherited. The question arises whether an older sedimentary or metamorphic event is responsible for this mixed age. Relics of a foliation (s_x) older than s_1 and s_2 , which are common throughout the Mount Wegener Nappe, were detected in thin sections of samples from this area. Schistosity

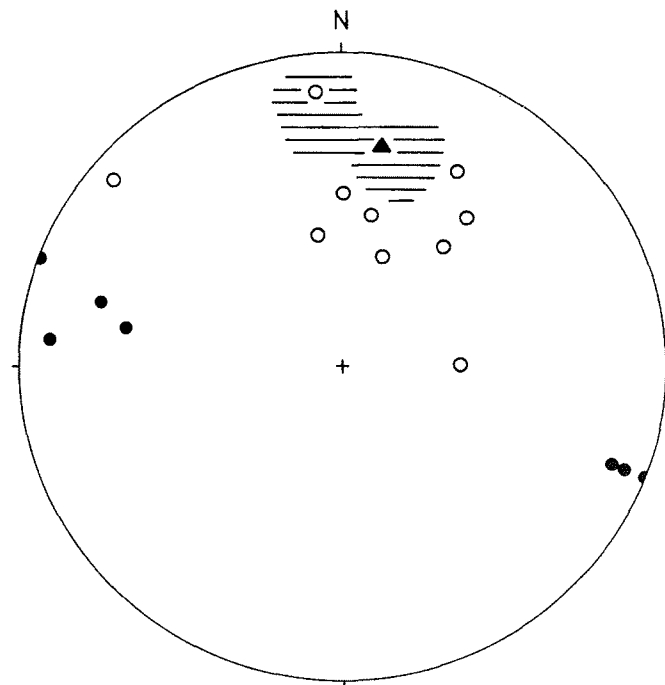


Fig. 23: Otter Highlands Thrust, near Y-Nunatak; Schmidt net diagram, showing incomplete rotation of B_1 axes (circles) into tectonic transport direction (shaded area, maximum = triangle); B_2 (dots) for comparison.

Abb. 23: Otter-Highlands-Überschiebung nahe Y-Nunatak. Dargestellt ist im Schmidtschen Netz die unvollständige Einrotation der B_1 -Achsen (Kreise) in die tektonische Transportrichtung (schraffierte Fläche, Maximum = Dreieck); B_2 (Punkte) zum Vergleich.

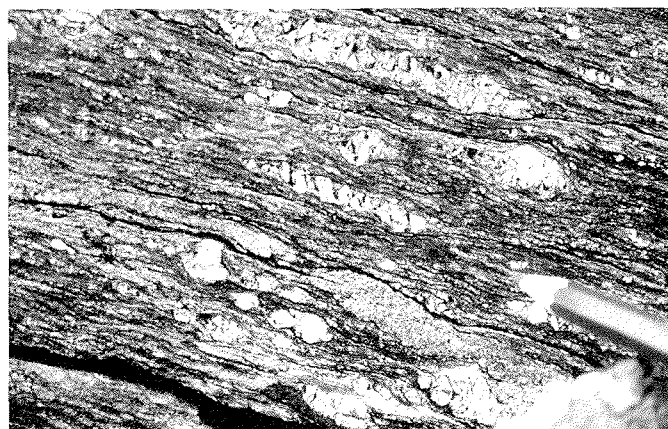


Fig. 24: Otter Highland Thrust, Y-Nunatak; mylonitized pegmatite; centre = feldspar showing book-shelf structure indicating southward displacement; left = south; right = north.

Abb. 24: Mylonitisierte Pegmatit, Otter-Highlands-Überschiebung, Y-Nunatak; In der Mitte = Feldspat mit Book-Shelf-Struktur als Beleg für Südschub des Hangenden; links = Süden, rechts = Norden.

s_x is probably an early relic of the Ross Orogeny, which led to the formation of s_1 and s_2 . On the other hand it could be possible that s_x is a relic of the same metamorphism which affected the rocks at Stephenson Bastion.



Fig. 25: Otter Highlands Thrust, Y-Nunatak; mylonitized pegmatite; centre = s-clast (feldspar) indicating southward displacement; left = south; right = north.

Abb. 25: Mylonitisierter Pegmatit, Otter-Highlands-Überschiebung, Y-Nunatak; In der Mitte = σ -Klast (Feldspat) als Beleg für Südschub des Hangenden; links = Süden, rechts = Norden

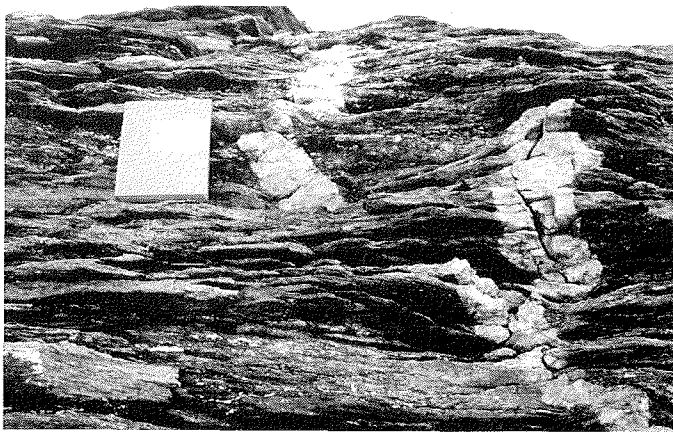


Fig. 26: Otter Highland Thrust, Y-Nunatak; offset of secondary pegmatite vein indicating southward displacement; left = south; right = north.

Abb. 26: Otter-Highlands-Überschiebung, Y-Nunatak; Versatz eines schmalen Pegmatitganges als Beleg für Südschub des Hangenden; links = Süden, rechts = Norden.

5. CONCLUSIONS

The Precambrian Read Group which is part of the East Antarctic Craton suffered metamorphism of regional scale about 1.6 Ga ago for the last time (REX 1972, HOFMANN et al. 1980, PANKHURST et al. 1983). The deeply eroded continental crust is unconformably overlain by Late Precambrian sediments of the Watts Needle Formation. Later metamorphism in the Read Group is restricted to distinct Ross aged shear zones. In the Watts Needle Formation very low-grade metamorphism was induced from the transported heat of the overlying Mount Wegener Formation. The transport of the Mount Wegener Nappe also led to deformation (e.g. folding, imbrication and cleavage) below its sole thrust during the Ross Orogeny.

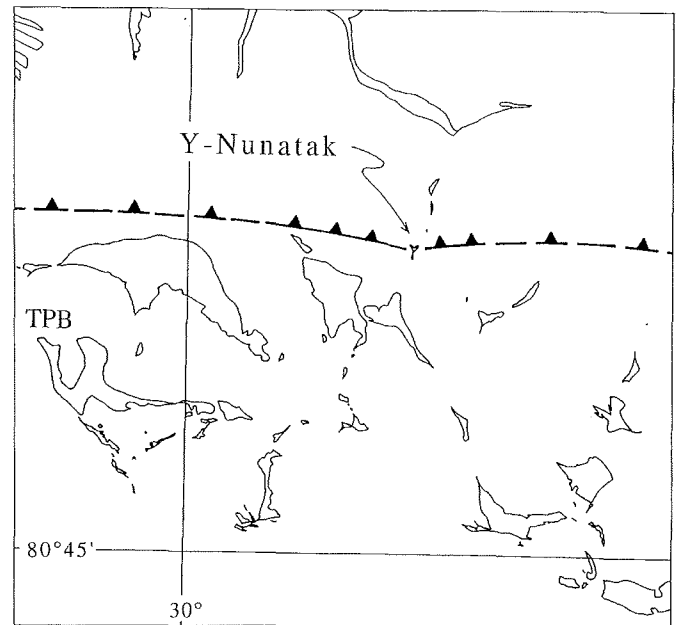


Fig. 27: Map of Turnpike Bluff area, southern Otter Highlands, showing the position of Y-Nunatak and of Otter Highlands Thrust. Coordinates taken from ANTARCTICA 1:250,000 (1983), TPB = Turnpike Bluff.

Abb. 27: Kärtchen der Turnpike-Bluff-Gegend (südliche Otter Highlands) mit der Lage des Y-Nunataks und der Otter-Highland-Überschiebung. Koordinaten nach ANTARCTICA 1:250.000 1983.

The former „Turnpike Bluff Group“ seems to consist of two separate rock units. The Stephenson Bastion Formation was probably deposited and possibly even metamorphosed about > 1250 Ma ago. We interpret the scattered K-Ar dates around 1 Ga to indicate a first low- to very low-grade metamorphism during Late Precambrian times. Only minor partial argon loss occurred during the Ross Orogeny at Stephenson Bastion, mainly at Clayton Ramparts. In the Wyeth Heights Formation, however, this Ross aged overprint resulted in growth of new biotite and reset the K-Ar clock. Nevertheless Rb-Sr dates and sedimentological arguments indicate that the Stephenson Bastion Formation and the Wyeth Heights Formation belong to one western rock unit.

The Mount Wegener Formation was deposited in a basinal environment during the Early Cambrian. It cannot be excluded that the sedimentation of this formation already started as early as Late Precambrian, but up to now there is no evidence for an age older than indicated by the Lower Cambrian fossils.

The relationship between the western rock units and the Mount Wegener Formation is not yet clear. We can only speculate that the Stephenson Bastion Formation might form the basement of the Lower Cambrian Mount Wegener Basin.

Independent of the stratigraphic relationships between the different formations of the former „Turnpike Bluff Group“, they acted as one structural unit when they were thrust southward over the East Antarctic Craton (Read Group) and its sedimentary cover (Watts Needle Formation) during the Ross Orogeny.

Towards the north medium- to high-grade metamorphic rocks of the Pioneer and Stratton Groups are thrust southward over the very low-grade to low-grade metasediments of the Mount Wege-ner Nappe.

ACKNOWLEDGEMENT

This work was supported by the „Deutsche Forschungsgemeinschaft“ (DFG, contracts KI 429/6 and Bu 312/14). Thanks also to the Bundesanstalt für Geowissenschaften und Rohstoffe (BGR), the Alfred-Wegener-Institut für Polar- und Meeresforschung (AWI), the British Antarctic Survey (BAS), and the crew of the supporting system. L. Thieswald and M. Metz conducted the argon analyses, H. Klappert did the potassium and Ar/Ar determinations, and H. Freitag (GKSS Geesthacht) carried out the neutron irradiation.

References

- Antarctica 1:250,000* (1983): Reconnaissance Series, SU 26–30/1* (20° W – 31° W), U.S. Dept. of the Int., Geol. Surv., Reston.
- Brauckmann, F.J.* (1984): Hochdiagenese im Muschelkalk der Massive von Bramsche und Vlotho.- Bochumer geol. geotechn. Arb. 14: 1-195, Bochum.
- Buggisch, W.* (1986): Diagenese und Anchimetamorphose aufgrund von Conodontenfarbe (CAI) und „Illit-Kristallinität“ (IC) - Methodische Untersuchungen und Daten zum Oberdevon und Unterkarbon der Dillmulde (Rheinisches Schiefergebirge).- Geol. Jb. Hessen, 114: 181-200, Wiesbaden.
- Buggisch, W., Kleinschmidt, G., Kreuzer, H. & Krumm, S.* (1990): Stratigraphy, metamorphism and nappe-tectonics in the Shackleton Range (Antarctica).- Geodät. Geophys. Veröffentlich., R. 1, 15: 64-86, Berlin.
- Buggisch, W., Kleinschmidt, G., Höhndorf, A. & Pohl, J.* (1994): Stratigraphy and facies of sediments and low-grade metasediments of the Shackleton Range, Antarctica.- Polarforschung 63: BL.
- Clarkson, P.D.* (1972): Geology of the Shackleton Range: A preliminary report.- Bull. Brit. Antarct. Surv. 31: 1-15, Cambridge.
- Clarkson, P.D.* (1982a): Geology of the Shackleton Range: I. The Shackleton Range Metamorphic Complex.- Bull. Brit. Antarct. Surv. 51: 257-283, Cambridge.
- Clarkson, P.D.* (1982b): Tectonic significance of the Shackleton Range.- In: CRADDOCK, C.(ed.), Antarctic Geoscience, 835-839, Madison.
- Clarkson, P.D.* (1983): Geology of the Shackleton Range: II The Turnpike Bluff Group.- Bull. Brit. Antarct. Surv. 52: 109-124, Cambridge.
- Frey, M.* (1987a) Very low-grade metamorphism of clastic sedimentary rocks.- In: FREY, M. (ed.), Low temperature metamorphism, 9-58, London.
- Frey, M.* (1987b): The reaction-isograd kaolinite + quartz = pyrophyllite + H₂O, Helvetic Alps, Switzerland.- Schweiz. Mineral. Petrogr. Mitt. 67: 1-11.
- Gerling, E.K., Levskii, L.K. & Morozova, I.M.* (1963): On the diffusion of radiogenic argon from minerals.- Geochemistry 6: 551-592.
- Gosen, W. von, Buggisch, W. & Krumm, S.* (1991): Metamorphism and deformation mechanisms in the Sierras Australes fold and thrust belt (Buenos Aires Province, Argentina).- Tectonophysics 185: 335-356, Amsterdam.
- Grikurov, G. E. & Dibner, A. F.* (1979): Vozrast i strukturnoe polozenie tolsk zapadnoj casti chrebita Sheklton (Antarktida).- Antarktika 18: 20-31.
- Hofmann, J., Kaiser, G., Klemm, W. & Paech, H.-J.* (1980): K/Ar-Alter von Doleriten und Metamorphiten der Shackleton Range und der Whichaway-Nunataks, Ost- und Südostumrandung des Filchner- Eisschelfs (Antarktis).- Z. geol. Wiss. 8: 1227-1232, Berlin.
- Hofmann, J. & Paech, H.-J.* (1983): Tectonics and relationships between structural stages in the Precambrian of the Shackleton Range, eastern margin of East Antarctic Craton.- In: OLIVER, R.L., JAMES, P.R. & JAGO, J.H. (eds.), Antarctic earth sciences, 183-189, Canberra.
- Hunziker, J.C.* (1987): Radiogenic isotopes in very low-grade metamorphism.- In: FREY, M. (ed), Low temperature metamorphism, 200-226, London.
- Hunziker, J.C., Frey, M., Clauer, N., Dalh Meyer, R.D., Friedrichsen, H., Flehmig, W., Hochstrasser, K., Roggwiler, P. & Schwander, H.* (1986): The evolution of illite to muscovite: mineralogical and isotopic data from the Glarus Alps, Switzerland.- Contrib. Mineral. Petrol. 92: 157-180.
- Jaboyedoff, M. & Thelin, P.* (1990): Preliminary note about illite Scherrer width in regard to preferred orientation.- TERRA Abstracts 3: 99.
- Kisch, H.J.* (1990): Calibration of the anchizone: a critical comparison of illite „crystallinity“ scales used for definition.- J. Metamorphic Geol. 8: 31-46.
- Kisch, H.J.* (1990): Illite „crystallinity“ recommendations on sample preparation, X-ray diffraction settings, and inter-laboratory samples.- J. Metamorphic Geol. 9: 665-670.
- Kleinschmidt, G., Buggisch, W. & Floettmann, T.* (1992): Compressional causes for the early Paleozoic Ross Orogen - evidence from Victoria Land and the Shackleton Range. - In: Y. YOSHIDA, K. KAMINUMA & K. SHIRAI-SCHI (eds.), Recent Progress in Antarctic Earth Science, 227-233, Tokyo.
- Klug, P.H. & Alexander, E. L.* (1974): X-ray Diffraction Procedures for Polycrystalline and Amorphous Materials.- John Wiley & Sons, New York-London-Sydney-Toronto.
- Krumm, S.* (1992): „Illitkristallinität“ als Indikator schwacher Metamorphose - Methodische Untersuchungen, regionale Anwendungen und Vergleiche mit anderen Parametern.- Erlanger Geol. Abh. 120, 74 pp.
- Krumm, S. & Buggisch, W.* (1991): Sample preparation effects on illite „crystallinity“ measurement: grain-size gradation and particle orientation.- J. Metamorphic Geol. 9: 671-677.
- Marsh, P. D.* (1983 a): The Late Precambrian and Early Palaeozoic history of the Shackleton Range, Coats Land.- In: OLIVER, R. L., JAMES, P.R. & JAGO, J. H. (eds.), Antarctic Earth Science, 190-193, Canberra.
- Marsh, P. D.* (1983 b): The stratigraphy and structure of the Haskard Highlands and Otter Highlands of the Shackleton Range.- Bull. Brit. Antarct. Surv. 60: 23-43, Cambridge.
- Merriman, R.J., Roberts, B. & Peacor, D.R.* (1990): A transmission electron microscope study of white mica crystallite size distribution in a mudstone to slate transitional sequence, North Wales, UK.- Contrib. Mineral. Petrol. 106: 27-40.
- Odin, G.S.* (ed.) (1982): Numerical dating in stratigraphy.- 630 pp., Chichester, J. Wiley & Sons.
- Paech, H.-J.* (1982): Als Geologe in den Read Mountains.- In: LANGE (ed.): Bewährung in Antarktika.- Antarktisforschung der DDR, 159-164, Leipzig.
- Paech, H.-J.* (1986): Vergleich der Entwicklung des südlichen Afrika mit der des antarktischen Kontinents.- Veröff. Zentralinst. Physik d. Erde 87: 1-205, Potsdam.
- Paech, H.-J., Meier, R., Hahne, K. & Vogler P.* (1987): The palaeoenvironment of the Riphean Turnpike Bluff Group sedimentation, Shackleton Range.- 5th Intern. Symp. Antarctic Earth Sci., Abstracts: 106, Cambridge.
- Paech, H.-J., Hahne, K. & Vogler, P.* (1991): Sedimentary environments of the Rhiphaen Turnpike Bluff Group, Shackleton Range.- In: THOMSON, M.R.A., CRAME, J.A. & THOMSON, J.W. (eds.), Geological Evolution of Antarctica, 123-128, Cambridge.
- Pankhurst, R.J., Marsh, P.D. & Clarkson, P.D.* (1983): A geochronological investigation of the Shackleton Range.- In: OLIVER, R.L., JAMES, P.R. & JAGO, J.B. (eds.), Antarctic Earth science, 176-182, Canberra.
- Reuter, A.* (1985): Korngrößenabhängigkeit von K-Ar Datierungen und Illit-Kristallinität anchizonaler Metapelite und assoziierter Metatuffe aus dem östlichen Rheinischen Schiefergebirge.- Göttinger Arb. Geol. Paläont. 27: 1-91, Göttingen.
- Rex, D.C.* (1972): K-Ar determinations on volcanic and associated rocks from the Antarctic Peninsula and Dronning Maud Land.- In: ADIE, R.J. (ed.), Antarctic Geology and Geophysics, 131-136, Oslo (Universitets-Forlaget).
- Seidel, E., Kreuzer, H. & Harre, W.* (1982): Late Oligocene/early Miocene high pressure belt in the external Hellenids.- Geol. Jb. E 23: 165-260, Hannover.
- Soloviev, I.A. & Grikurov, G.E.* (1979): Prevye nachdokie sredned kembiriskich-trilobitov v chrebita Sheklton (Antarktida).- Antarktika 17: 187-203.
- Steiger, R.H. & Jäger, E.* (1977): Subcommission of geochronology: convention on the use of decay constants in geo- and cosmochronology.- Earth Planet. Sci. Lett. 36: 359-326.
- Voll, G.* (1960): New work on petrofabrics.- Liverpool and Manchester Geol. J. 2: 503-567, Liverpool.

Warr, L.N. & Rice, A.H.N. (1994): Interlaboratory standardization and calibration of clay mineral crystallinity and crystallite size data.- J. Metamorphic Geol. 12: 141-152.

Weber, B. (1991): Microfossils in Proterozoic sediments from the southern Shackleton Range, Antarctica: a preliminary report.- Z. geol. Wiss. 19: 185-197, Berlin.